

## Review

# Spatial oncology: Translating contextual biology to the clinic

Dennis Gong,<sup>1,2,3,6</sup> Jeanna M. Arbesfeld-Qiu,<sup>1,2,4,5,6</sup> Ella Perrault,<sup>1,2,4,5,6</sup> Jung Woo Bae,<sup>1,2</sup> and William L. Hwang<sup>1,2,4,5,\*</sup>

<sup>1</sup>Center for Systems Biology, Department of Radiation Oncology, Center for Cancer Research, Massachusetts General Hospital, Boston, MA, USA

<sup>2</sup>Broad Institute of MIT and Harvard, Cambridge, MA, USA

<sup>3</sup>Massachusetts Institute of Technology, Cambridge, MA, USA

<sup>4</sup>Harvard University, Graduate School of Arts and Sciences, Cambridge, MA, USA

<sup>5</sup>Harvard Medical School, Boston, MA, USA

<sup>6</sup>These authors contributed equally

\*Correspondence: [whwang1@mgh.harvard.edu](mailto:whwang1@mgh.harvard.edu)

<https://doi.org/10.1016/j.ccel.2024.09.001>

## SUMMARY

Microscopic examination of cells in their tissue context has been the driving force behind diagnostic histopathology over the past two centuries. Recently, the rise of advanced molecular biomarkers identified through single cell profiling has increased our understanding of cellular heterogeneity in cancer but have yet to significantly impact clinical care. Spatial technologies integrating molecular profiling with microenvironmental features are poised to bridge this translational gap by providing critical *in situ* context for understanding cellular interactions and organization. Here, we review how spatial tools have been used to study tumor ecosystems and their clinical applications. We detail findings in cell-cell interactions, microenvironment composition, and tissue remodeling for immune evasion and therapeutic resistance. Additionally, we highlight the emerging role of multi-omic spatial profiling for characterizing clinically relevant features including perineural invasion, tertiary lymphoid structures, and the tumor-stroma interface. Finally, we explore strategies for clinical integration and their augmentation of therapeutic and diagnostic approaches.

## INTRODUCTION

For almost two hundred years since Johannes Müller published the first studies of tumors examined by light microscopy,<sup>1</sup> cancers have been researched in the lab and diagnosed in the clinic using histological sections of tissue. Visualization of cancer cells and the tumor microenvironment (TME) using marker-specific and morphologic staining has transformed our understanding of disease progression from benign lesions to invasive malignancy. Our understanding of the spatial organization of tumor cells has answered key questions about interactions with the immune system,<sup>2</sup> remodeling of stromal cells to support growth,<sup>3</sup> and the subclonal heterogeneity<sup>4</sup> present in spatial niches.

More recently, with the rise of next-generation sequencing (NGS) and the comprehensive molecular characterization of tumor genetics it has provided, the landscape of cancer diagnostic technologies and tumor targeted therapies has progressed rapidly.<sup>5</sup> The development of spatial molecular profiling technologies in the past several years has capitalized on the value of this molecular information, placing many important discoveries into tissue context and answering critical questions relating to treatment resistance, tumor heterogeneity, and clonal evolution.

These advances will continue to mature as spatial technologies and workflows used to collect these measurements improve in quality, scale and accessibility. However, the clinical impact of these high-dimensional approaches remains unclear. Currently actionable diagnostics and therapeutics have been identified in

an era where these technologies did not exist, and it remains to be proven what novel discoveries can be made uniquely from spatial molecular profiling. Furthermore, integration of spatial assays into clinical care will inevitably face challenges, including costly prospective clinical validation studies, bioinformatics tools to synthesize large and complex datasets in clinical practice, and more streamlined and high throughput workflows than what the current generation of technologies provides.<sup>6</sup> This review addresses the immense translational opportunity for spatial profiling technologies to impact clinical care and enable precision medicine in oncology. We cover (1) extant spatial technologies that have been applied to clinical samples; (2) therapeutic strategies for targeting multicellular interactions identified using spatial profiling; (3) spatial biomarker identification and validation in clinical cohorts; and (4) strategies for integrating spatial insights into the clinic. We conclude with a perspective on how the future of spatial profiling technologies and studies will impact patient care.

## HISTORY OF SPATIAL TECHNOLOGIES IN ONCOLOGY

### *In situ* cancer diagnostics

The development of spatial profiling technologies builds upon pioneering advances in molecular biology and imaging. Routine clinical hematoxylin and eosin (H&E) staining of formalin-fixed and paraffin-embedded (FFPE) tumor sections can resolve the *in situ* locations of hundreds of thousands of cells along with



morphological details that can be used to annotate cell types and architectural features. More specialized staining using immunohistochemistry (IHC) for specific protein targets or fluorescence *in situ* hybridization (FISH) for detecting chromosomal translocations are also routinely performed in histopathology diagnostic workflows.

These assays can serve several purposes. Pathological review of H&E<sup>7</sup> based upon morphological and spatial features of tumor cells in relation to stroma and normal tissue have been used to stage tumors, provide prognostic information, and guide therapeutic decision making. Following surgery, assessment of tumor involvement at surgical margins can influence adjuvant therapy decisions. Finally, examining the TME following therapy can evaluate responsiveness to treatment and characterize residual treatment-resistant cells.

More recently, specific histological assays have been used as companion diagnostics to directly guide the choice of therapy or enrich for certain tumor characteristics in clinical trials. For example, patients receiving immune checkpoint blockade (ICB) are routinely assessed for PD-L1 protein expression by IHC, which can stratify patients and exclude those unlikely to benefit.<sup>8</sup> Other antibody-based therapies use IHC tissue diagnostics in a similar manner to identify eligible patients. The HercepTest is a tissue diagnostic test that was co-approved with the HER2 antibody trastuzumab, and more recently, a folate receptor alpha (FR $\alpha$ ) IHC assay was approved to define eligible patients for a FR $\alpha$  directed antibody drug conjugate.<sup>9</sup> Finally, additional IHC assays that characterize mismatch repair status<sup>10</sup> (MMR proteins) or mitotic rate<sup>11</sup> (Ki67 positivity) have been utilized to select eligible patients for specific therapies.

### Bringing molecular multiplexing to the clinic

Singular or lowly multiplexed molecular profiling has clear clinical utility, but the complexity of tumor tissues may require more comprehensive assessment of molecular details to fulfill the promise of precision oncology. In an ideal world, clinicians and researchers would be able to utilize scarce clinical tissues and make comprehensive molecular measurements that can be used to inform clinical decision making. However, current tissue analysis solutions must make tradeoffs between molecular phenotyping depth, cellular resolution, and spatial context that limit new biomarker development.

Historically, bulk tumor profiling methods have provided sensitive detection of molecular biomarkers at broad coverage, but at the expense of cellular resolution. Clinically, these assays are typically performed by dissociating frozen, fixed, and FFPE-preserved specimens and then purifying the nucleic acid contents of the sample. These molecular assays for tumor genotyping have enabled precise characterization of tumor biology and enabled the development of new companion diagnostics.<sup>12</sup> For example, a comprehensive tissue-based multi-tumor genotyping panel examines DNA mutations in 324 genes that may stratify responses to treatment with 28 approved targeted therapies.<sup>13</sup> Targeted RNA expression and DNA methylation assays have also been widely commercialized and help providers provide prognostic information such as likelihood of tumor recurrence,<sup>14</sup> risk of metastasis,<sup>15</sup> or response to therapy.<sup>16–18</sup> Other commercial providers use whole exome sequencing or whole transcriptome sequencing to identify genomic signatures such as homologous

repair deficiency, genomic loss of heterozygosity, microsatellite instability, tumor mutation burden, and other genomic alterations (e.g., copy number variation, chromosome rearrangements, alternative splicing, and transcriptional subtype signatures) that stratify response to certain therapies.<sup>19–21</sup> Finally, liquid biopsies have also been used to generate molecular profiles of tumor clonality and response to therapy, including circulating tumor DNA, plasma protein, cell free RNA, and circulating cell based biomarkers.<sup>22,23</sup>

Bulk and ensemble-based methods of tumor profiling have become a stalwart of the pathological workup of many tumors but are inherently limited by two factors: non-malignant dilution of tumor specific signals and lack of spatial resolution. While various computational methods have been developed to deconvolute cell type specific expression from bulk data,<sup>24</sup> in practice the results can be highly variable depending on tissue origin and sample composition.<sup>25</sup> Laser capture microdissection protocols can be used to selectively enrich tumor cells but throughput is low and limited tissue material can be collected from a single section.<sup>26</sup> Single cell sequencing approaches address one of these factors by providing broad molecular depth with single cell resolution, to enable high throughput cell type specific assignment of molecular biomarkers. The technological and throughput advances of single cell sequencing has showcased the importance of heterogeneity in the TME and led to the discovery of cell type specific biomarkers, novel cellular states, and rare cell types, reviewed comprehensively elsewhere.<sup>27,28</sup> However, the dissociative techniques that underlie single cell sequencing protocols require a large amount of input material<sup>29</sup> making them in practice difficult to perform with clinical tissues. The lack of spatial context can also make it difficult to interpret aspects of the resulting datasets, such as cell-cell communication and spatial organization of cell types.<sup>30</sup>

### Commercial spatial analysis systems

Spatially resolved multiplexed assays are now being developed and commercialized to bridge the gap between comprehensive molecular profiling and spatial tissue context in clinical specimens. These high-plex molecular assays are tractable with low tissue input and can provide high sensitivity measurements of a variety of analytes that can augment existing histology workflows in a spatially preserved manner.

For large primary resections, spatial technologies can chart the structural features in the microenvironment that contribute to heterogeneity in immune infiltration and treatment sensitivity. In cases where only a few cells are analyzed, such as when sampling lymph node micrometastases, identifying early-stage invasion amid substantial background inflammation, or examining tumors with low cellularity, the ability to detect a multitude of biomarkers *in situ* with high sensitivity is clinically important. This capability is unachievable with technologies that necessitate cell dissociation, like DNA sequencing or single-cell RNA sequencing (scRNA-seq).<sup>29,31</sup> Additionally, molecular information can augment interpretation of histological features that have indeterminate characterization from non-specific staining. The presence of complex features including composition of infiltrating immune cells, desmoplasia, tumor budding, and entosis have for decades demonstrated associations with clinical phenotypes but have yet to be utilized in diagnostic or prognostic workflows to date.<sup>32–35</sup> For

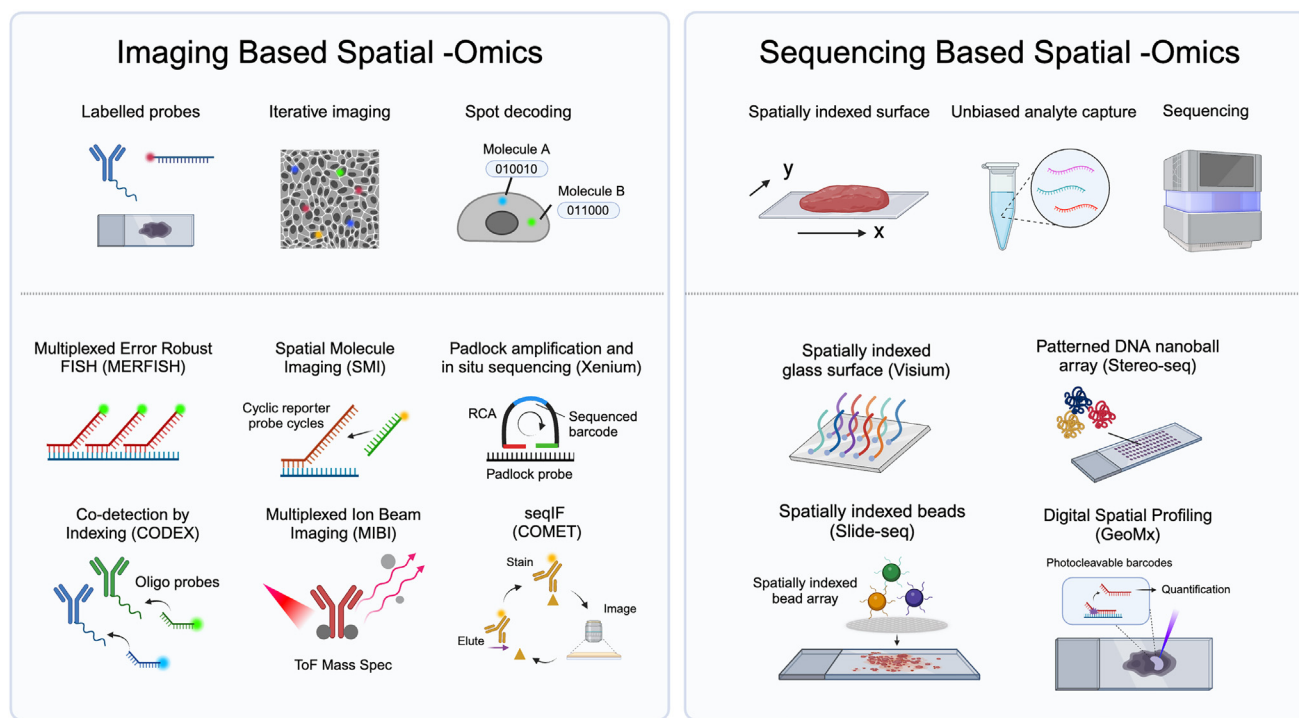


**Figure 1.** Schematic depiction of commercial spatial technology platforms

example, transcript or protein based subtyping of infiltrating immune cells can differentiate regulatory versus effector T cell infiltrates that have distinct prognostic value.<sup>36</sup>

Commercially available spatial platforms largely segregate into imaging or sequencing based tools and have focused primarily on RNA and protein as detected analytes (Figure 1). Various systems have each been subjected to benchmarking by the broader research community, revealing distinct advantages and tradeoffs of each technology. Considerations include not only experimental parameters such as spatial resolution, sensitivity/specifity tradeoffs, and molecular plex, but also practical factors such as experimental cost, acquisition times, and complexity of analysis workflows. Imaging-based methods offer high levels of spatial precision and relatively higher sensitivity and specificity compared to sequencing-based platforms, at the tradeoff of lower molecular plex, longer acquisition times, and escalating costs with increasing plex. Conversely, sequencing based methods can provide more unbiased coverage at lower prices and higher throughput, providing an advantage for exploratory applications.

The widespread adoption of these platforms has rapidly grown over the past 5 years. Multiplexed proteomics technologies were the first to achieve commercial usage, first with low-plex solutions such as the Opal 6-plex Vectra Polaris instruments, and now with barcode based approaches such as co-detection by indexing (CODEX) that can reach over 100-plex in a single tissue section.<sup>37</sup> In contrast to these imaging-based approaches for proteomics, the initial commercial rollout of spatial RNA profiling systems was largely dominated by discovery approaches with transcriptome wide coverage (e.g., spatial transcriptomics and digital spatial profiling) at the tradeoff of spatial resolution. Multi-

plexed RNA imaging based spatial profiling enabled by probe based barcoding schemas quickly followed discovery-based approaches, providing subcellular spatial resolution of transcripts, albeit with fewer target genes. In recent years, imaging-based approaches have expanded their target coverage to thousands of targets while unbiased discovery focused approaches like spatial transcriptomics have increased their spatial resolution. A summary of these commercial platforms is presented in Table 1.

Emerging technologies such as same slide multi-omics<sup>38–40</sup> have refined our ability to resolve complex tissue phenotypes. Spatial epigenomics, metabolomics, and genomics technologies are also maturing but have thus far been restricted primarily to proof-of-concept studies without commercialization or widespread use on clinical samples. Spatial proteomics and transcriptomics have dominated spatial applications in clinical tissue. Importantly, academic- and industry-led upgrades to these technologies are continually occurring, leading to improvements in sensitivity, molecular plex, and accuracy. In addition, there is considerable development of new approaches in both the academic and industry settings. Recently, sequencer based approaches that adapt flow cells used in NGS to resolve spatial locations of transcripts have combined the resolution of imaging based systems with the flexibility of high plex or potentially unbiased analyte detection.<sup>41</sup> These systems, including the recently commercialized G4X Spatial Sequencer, have appeal for clinical applications due to their large imaging area and high throughput.

#### Computational methods for spatial data analysis

Concurrent with the rise of spatial measurement technologies has been the rapid development of computational tools and

**Table 1. Commercial spatial technologies in the clinic**

| Commercial name | Technology platform  | Molecular plex <sup>a</sup>                 | Predicate academic work   |
|-----------------|--|---|---|
| CosMx           | CosMx SMI utilizes hybridization probes with multiple branched readout sequences to bind mRNA targets. Reporter probes then bind to readout sequences to decode the identity of the molecule. While initially commercialized for spatial transcriptomics as the CosMx platform, SMI enables the detection of RNA or protein analytes, as antibody probes can also be labeled with branched readout barcodes. CosMx provides high sensitivity detection of fairly degraded/fragmented RNA.  | >18,000 RNA targets                         | Spatial molecular imaging <sup>182</sup>  |
| Xenium          | The Xenium platform utilizes a combination of technologies, namely padlock probe amplification, followed by fluorescence <i>in situ</i> sequencing (FISSEQ) to achieve high sensitivity detection of RNAs. Padlock probes bind two nearby sites on an RNA molecule anneal and amplify a barcode sequence via rolling circle amplification, which is readout using cyclic <i>in situ</i> sequencing.  | 5000-plex RNA                               | FISSEQ <sup>183</sup><br>Padlock probe <i>in situ</i> sequencing <sup>184</sup> |
| MERSCOPE        | MERSCOPE reads out the location of RNA using multiple hybridization probes that bind distinct sites on a single RNA molecule. Each probe contains a separate readout sequence that binds distinct reporter probes, and the combination of reporter probes that bind to each RNA can be used to identify the RNA species in an error robust manner.   | 1000-plex RNA                               | MERFISH <sup>185</sup>  |
| Visium          | The spatial transcriptomics (ST) approach, now commercialized as Visium, uses 50 micron diameter “spots” containing spatially barcoded 3' mRNA capture sequences arrayed on a tissue capture area. Each capture sequence encodes a spatial barcode that can be resolved by NGS to reconstruct spatial location. Recently, a higher resolution version of the technology termed Visium HD has been developed which further improves the spot resolution to 2 × 2 μm squares, providing higher sensitivity detection, improved spatial resolution, and complete tiling over the tissue without gaps between spots. | Unbiased coverage of all 3' tagged mRNA     | Spatial transcriptomics <sup>186</sup>  |
| Stereo-seq      | Stereo-seq (spatial enhanced resolution omics-sequencing) uses patterned DNA nanoball arrays to achieve small spot size (500 nm resolution) and large capture area (up to 13.2 × 13.2 cm for fresh frozen tissue; 1 × 1 cm for FFPE). 3' mRNA capture sequences enable a sequencing based readout to spatially assign transcripts.   | Unbiased coverage of all 3' tagged mRNA     | Stereo-seq <sup>142,187</sup>   |
| Seeker          | Seeker utilizes the Slide-SeqV2 technology that leverages patterned bead arrays (10 μm resolution) engineered with spatial barcodes and a 3' capture sequence. Seeker is not currently compatible with FFPE tissues.   | Unbiased coverage of all 3' tagged mRNA     | Slide-seqV2 <sup>188</sup>  |
| GeoMx           | GeoMx digital spatial profiling (DSP) achieves spatial resolution using mRNA or protein specific probes that contain photocleavable oligonucleotide tags. Projected UV light is applied in a spatially controlled manner that releases the oligo tags to be then captured by microcapillary aspiration and sequenced or counted to quantify abundance.   | >18,000 RNA targets or >570 protein targets | Digital spatial profiling <sup>189</sup>  |
| PhenoCycler     | The co-detection by indexing (CODEX) technology underlying the PhenoCycler platform is a cyclic immunofluorescence based assay that can image tens to more than a hundred protein targets. Multiplexed analysis of proteins is made possible using <i>in situ</i> hybridization of fluorescent probes that hybridize to index barcodes tagged to antibodies.   | Up to 103-plex                              | CODEX <sup>190</sup>  |

(Continued on next page)

**Table 1. Continued**

| Commercial name | Technology platform  | Molecular plex <sup>a</sup> | Predictive academic work     |
|-----------------|--|-----------------------------|------------------------------|
| COMET           | COMET utilizes sequential immunofluorescence (seqIF) to perform up to twenty cycles of staining, imaging, and elution for multiplexed protein detection. The advantage of such a platform is the miniaturization and speed offered by microfluidics, as well as the ability to use off-the-shelf primary antibodies without conjugation.   | Up to 40-plex               | seqIF <sup>191</sup>         |
| MIBIscope       | Multiplexed ion beam imaging (MIBI) uses metal labeled antibodies in conjunction with highly sensitive Secondary Ion Mass Spectrometry to enable highly multiplexed detection of protein targets.  | Up to 40-plex               | MIBI <sup>63</sup>           |
| CellScape       | The CellScape assay uses standard commercially available fluorescently labeled antibodies and iterative cycles of staining, imaging, bleaching, and background subtraction to quantify staining intensity. In contrast to other technologies, the automated ChipCytometry platform requires tissue loading directly on a glass coverslip, which is then loaded into a microfluidic chip apparatus. | Up to 30-plex               | ChipCytometry <sup>192</sup> |

<sup>a</sup>Molecular plex benchmarks refer to what has been experimentally demonstrated thus far in publicly available publications. The theoretical limit is higher.

pipelines for data processing and analysis. While several reviews<sup>42,43</sup> have been published that comprehensively describe the landscape of these methods, this section highlights specific concepts important for interpreting data from spatial assays in clinical settings. These include tools for cell segmentation, methods for building single cell profiles in space, and algorithms for deconvolution of tumor heterogeneity.

In imaging-based approaches, cell segmentation from morphology markers (e.g., cell membrane and nuclear staining) is a critical first step for constructing accurate single cell profiles. Machine learning algorithms such as CellPose<sup>44</sup> and StarDist<sup>45</sup> trained on manually curated segmentation examples, often provide serviceable first-pass results. However, the diversity of tissue architectures and cell shapes makes some degree of error unavoidable. Substantial effort has also been dedicated to mapping these spatial profiles to reference atlases,<sup>46</sup> facilitating the integration of spatial information with single-cell data. For example, the development of STELLAR, a geometric deep learning method by Brbić et al., enables the automated annotation of cells across different tissues and diseases.<sup>47</sup> Using spatially resolved single-cell datasets, STELLAR learns the spatial and molecular similarities of single cells, along with their neighborhood composition and structure, then scores the cells as either matching annotated reference sets or as novel cell types or states.

In sequencing-based approaches, the resolution is constrained by spot size. Even at subcellular resolution, accurate segmentation is challenging due to overlapping cells and transcript diffusion during tissue processing. Thus, statistical algorithms capable of deconvolution and error correction have greatly enhanced the interpretability of spatial profiling assays. These methods such as robust cell type decomposition (RCTD)<sup>48</sup> often utilize single cell atlasing efforts, learning typical single cell profiles, matching them to spatially assigned spots, and correcting misassigned transcripts. More recently, integrated approaches<sup>49</sup> utilizing subcellular sequencing-based methods have refined predicted cell annotations to the subcellu-

lar spot level. For imaging-based approaches, methods like Bayso<sup>50</sup> assign cell types based on spatial location of individual transcripts, thus bypassing the need for cellular segmentation.

After cell type annotation, many of the basic analytical approaches for analyzing single cell data can be applied to study tumor heterogeneity while integrating spatial information. These include basic approaches, such as hierarchical clustering to identify subpopulations of cell types within tumors, and topic modeling approaches, such as consensus non-negative matrix factorization (cNMF),<sup>51</sup> that identify shared gene programs corresponding to specific cellular functions. Finally, spatially variable expression algorithms are applied to identify differentially expressed genes across locations and biomarkers with spatially restricted expression. Visualizing expression gradients can elucidate the effects of TME features such as hypoxia, immune aggregates, and the tumor invasive front (TIF), as detailed in subsequent sections. Furthermore, advanced algorithms that infer specific cellular interactions hold significant translational potential and are discussed in later sections. Importantly, benchmarking studies serve as a crucial resource for biologists, helping to contextualize and understand the distinct advantages and use cases of various algorithms in this rapidly evolving field.

## THERAPEUTICALLY TARGETING CELLULAR INTERACTIONS IN THE TUMOR MICROENVIRONMENT

Tumor heterogeneity poses a significant obstacle to the efficacy of cancer therapies.<sup>52–54</sup> While targeted therapy has transformed clinical management of certain molecularly characterized subtypes of cancer, subclones of cells within the heterogeneous tumor can maintain or develop resistance to targeted therapy, rendering treatment ineffective over time. Targeting a broader network of cellular interactions to generate endogenous anti-cancer mechanisms within the TME may provide an orthogonal and more systematic means of tumor clearance.<sup>55–58</sup> Advances in spatial transcriptomic technology have enabled greater investigation into the architecture and function of heterogeneous

**Table 2.** Summary of selected studies that use spatial transcriptomics to identify biomarkers of prognosis or response to treatment

| Spatial Biomarker                           | Cancer type                      | Clinical correlation   | Reference  |
|---|----------------------------------|--|--|
| Predicting response to immunotherapy        |                                  |  |  |
| Infiltration of specific immune cell states | Non-small cell lung cancer       | Developed SpatialVizScore with ability to differentiate an “immune-suppressed” state with high immune cell infiltration that expresses immunosuppressive ligands.  | Allam et al. <sup>118</sup>  |
|   | Glioblastoma                     | Cellular neighborhood containing MPO+ macrophages is correlated with long-term survival.   | Karimi et al., 2023 <sup>122</sup>   |
|   | Cutaneous T cell lymphoma        | Developed SpatialScore, which calculates the physical distance ratio of each CD4 <sup>+</sup> T cell and its nearest tumor cell relative to its nearest Treg and was predictive of response to pembrolizumab.  |  |
|   | Pancreatic ductal adenocarcinoma | Developed a spatial proximity score (imRS) that measures distance of CD4 <sup>+</sup> T cells to IL10+ myelomonocytes and GZMB+ CD8 <sup>+</sup> T cells and found this signature was significantly enriched in long-term survivors.   | Mi et al. <sup>119</sup>   |
|   | Non-small cell lung cancer       | CD163+ macrophage infiltration is driven by upregulation of <i>CD27</i> , <i>ITGAM</i> , and <i>CCL5</i> in malignant cells and is associated with worse clinical outcomes.  | Larroquette et al. <sup>193</sup>  |
|   | Breast cancer                    | Responders to pembrolizumab in triple negative breast cancer (TNBC) formed two groups: one showing antitumor immunity before treatment (high MHC expression, presence of TLS) and the other with nonresponders at baseline followed by a strong immune response (cytotoxic T cells and antigen presenting myeloid cells infiltration). Nonresponders were characterized by lack of immune infiltrate before and after therapy. Another study found 3 spatial immunophenotypes in response to anti-PD1 treatment in TNBC: an “excluded” and “ignored” phenotype that do not respond to ICB and related to TGF- $\beta$ /VEGF pathways and the WNT/PPAR- $\gamma$ pathways, respectively; as well as an “inflamed” phenotype associated with response to ICB with high infiltration of CLEC9A + dendritic cells. | Shiao et al. <sup>120</sup><br>Hammerl et al. <sup>194</sup>                               |
| Spatially localized gene expression         | Breast cancer                    | Intraepithelial PD-L1 expression is correlated with increased recurrence-free survival, while peritumoral stromal PD-L1 expression is correlated with worse prognosis and T-reg infiltration. High fraction of CD8+/TCF1+ T cells and MHC/I/II + cancer cells were the best predictors of response to neoadjuvant immune checkpoint blockade (ICB) in TNBC.  | Carter et al. <sup>131</sup><br>Gruoso et al. <sup>130</sup><br>Wang et al. <sup>195</sup> |
|   | Melanoma                         | PD-L1 expressed on macrophages, but not tumor cells, is associated with increased overall survival, progression free survival, and response to ICB.  | Toki et al. <sup>132</sup>   |

(Continued on next page)

**Table 2. Continued**

| Spatial Biomarker   | Cancer type                                   | Clinical correlation   | Reference   |
|---|---|--|---|
|   | Non-small cell lung cancer                    | CD44 expressed in tumor cells, but not immune cells, is associated with greater progression free survival under PD-L1 blockade. <i>CSF1R</i> expression in malignant cells is associated with greater progression-free survival and overall survival under ICB.  | Moutafi et al. <sup>196</sup><br>Larroquette et al. <sup>193</sup>    |
|   | Head and neck squamous cell carcinoma (HNSCC) | Responders to immunotherapy compared to nonresponders were found to have higher expression of PDL1, B7-H3, and OX40L/CD252 in the tumor; lower expression of VISTA and FOXP3 in the tumor; and higher expression of B7-H3, CD40, and CD27 in the stroma.   | Sadeghirad et al. <sup>197</sup>                                      |
| Spatial organization of immune cells as biomarkers of prognosis and response to treatment |   |  |   |
| Immunity hubs   | Non-small cell lung cancer                    | Cellular neighborhoods enriched in B cells and CD4 <sup>+</sup> T cells were associated with increased overall survival.   | Sorin et al. <sup>136</sup>   |
|   | Melanoma<br>Urothelial cancer<br>HNSCC        | Shorter distance between CD8 <sup>+</sup> T cells and cancer cells and macrophages and cancer cells is associated with a favorable response to ICB.  | Moldoveanu et al. <sup>135</sup><br>Gil-Jimenez et al. <sup>198</sup> |
|   | Breast cancer                                 | Cancer cell-B cell interactions and cancer cell-CD8 <sup>+</sup> GZMB+ T cell interactions were top predictors of response to neoadjuvant ICB in TNBC.   | Wang et al. <sup>195</sup>  |
|   | Glioblastoma                                  | Enrichment of activated T cells and macrophages in perivascular regions is associated with a “long-term survival” cohort.  | Alanio et al. <sup>134</sup>  |
|   | Colorectal cancer                             | Identified hubs of malignant cells expressing interferon response genes and activated (CXCL13+) T cells maintained by CXCR3 ligands that induce IFN- $\gamma$ in T cells to recruit additional T cells.  | Pelka et al. <sup>133</sup>   |
|   | Pancreatic ductal adenocarcinoma              | Presence of lymphoid aggregates of B cells and CD8 <sup>+</sup> T cells is significantly higher in long-term survivors.  | Mi et al. <sup>119</sup>  |
|   | Hepatocellular carcinoma (HCC)                | Immunosuppressive B cells infiltrate WNT wild-type metastatic tumors, inducing terminal exhaustion of CD8 <sup>+</sup> T cells through a NKG2A checkpoint pathway and nonresponse to anti-PD1 therapy.   | Sun et al. <sup>199</sup>   |
| Tertiary lymphoid structures (TLS)  | Breast cancer<br>Melanoma                     | Identification of a transcriptomic signature of TLS; application of this signature to bulk RNA sequencing datasets of melanoma was predictive of overall survival.   | Andersson et al. <sup>137</sup>                                       |
|   | Hepatocellular carcinoma                      | Identified a 50-gene signature of TLS (TLS-50) from spatial transcriptomic data; TLS-50 scores in bulk transcriptomic data of HCC samples were significantly associated with better prognosis.   | Wu et al. <sup>74</sup>   |
|   | Renal cell carcinoma                          | TLS contain CD4 <sup>+</sup> T cells and plasma cells that promote B cell differentiation, highlighting the role of TLS as an intratumoral source of antibody-producing cells. Furthermore, TLS+ tumors are associated with higher frequency of apoptotic malignant cells and greater therapeutic response and progression free survival in patients treated with ICB. | Meylan et al. <sup>138</sup> , Liu et al. <sup>139</sup>              |

(Continued on next page)

**Table 2. Continued**

| Spatial Biomarker   | Cancer type   | Clinical correlation   | Reference   |
|---|---|--|---|
| Identification of and cell states at the tumor invasive front (TIF) |   |  |   |
| Identification of the TIF   | Prostate cancer   | Conducted factor analysis to identify transcriptomic modules corresponding to normal glands, cancer, and prostatic intraepithelial neoplasia and found that the cancer module is also expressed outside of the normal tumor boundary.  | Berglund et al. <sup>146</sup>                          |
|   | Pancancer   | Cotrazm is a computational tool to delineate the tumor boundary by integrating spatial location and inferred copy number variants from spatial transcriptomic data.  | Xun et al. <sup>147</sup>                               |
|   | Oral squamous cell carcinoma                                | Cancer cells at the leading edge expressed modules related to cell cycle, epithelial-mesenchymal transition (EMT), and angiogenesis. Furthermore, this “leading-edge” gene signature was related to worse disease specific survival and progression-free interval when applied to bulk transcriptomic data of multiple cancer types.   | Arora et al. <sup>143</sup>                             |
| Cell states and communities at the TIF                              | Hepatocellular carcinoma<br>Intrahepatic cholangiocarcinoma | Hepatocytes at the TIF have higher expression of serum amyloid A1 and A2 and higher expression of these proteins at the tumor margin is significantly associated with worse overall survival and the recruitment and polarization of M2 macrophages. Niches of PROM1+/CD47+ cancer stem cells are identified at the TIF and malignant cells at the TIF had increased expression of EMT programs. | Wu et al. <sup>74</sup> ; Wu et al. <sup>142</sup>      |
|   | Melanoma  | Cytokine gradients induced by the JAK-STAT-IDO1 pathway maintain communities of suppressive T-reg and PD-L1 myeloid cells at the TIF.  | Nirmal et al. <sup>200</sup>                            |
|   | Breast cancer   | Malignant cells at the TIF in breast cancer upregulate the oxidative phosphorylation pathway in early dissemination and higher expression of genes involved in this pathway is associated with worse clinical outcomes. In lung metastases, TREM2+ macrophages are enriched at the metastatic TIF, promoting an immunosuppressive niche.   | Liu et al. <sup>144</sup><br>Yofe et al. <sup>201</sup> |
|   | Colorectal cancer   | Metabolically inactive CD39/PD1+ T cells are excluded from the tumor-immune boundary, while metabolically active CD39/PD1+ T cells are more proximal to the boundary.  | Hartmann et al. <sup>141</sup>                          |
|   | Renal cell carcinoma  | EMT gene expression program is enriched at the TIF and colocalized with IL1B+ macrophages.   | Li et al. <sup>202</sup>                                |

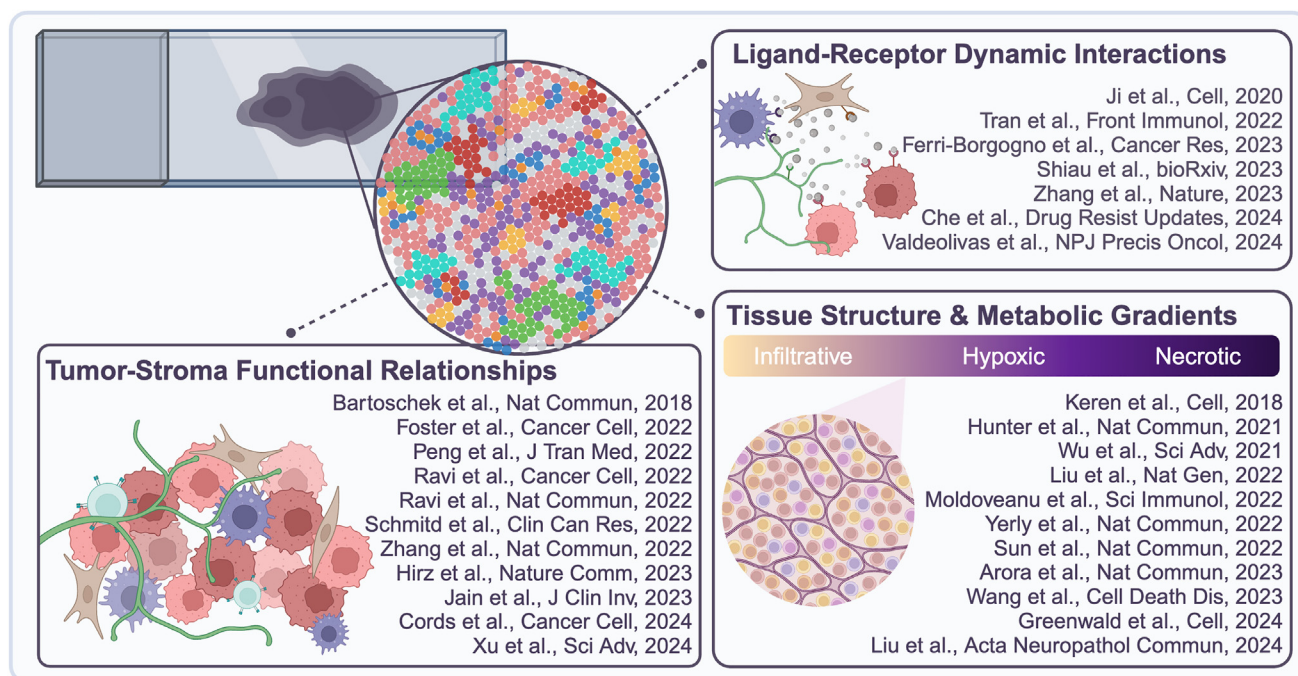


**Figure 2.** Spatial technology identifies multicellular interactions in the TME

multicellular interactions in TMEs.<sup>59–62</sup> The following examples illustrate ways in which spatial transcriptomics can be utilized in preclinical studies to identify relevant cellular interactions in the TME to be further investigated for therapeutic targeting (Figure 2).

#### Neighborhood analysis of multicellular ecosystems

Neighborhood analysis is an approach used to characterize the cellular composition of spatially defined microenvironments and can be applied to study how the spatial organization of cells leads to emergent properties relevant to disease progression.<sup>63–67</sup> High-resolution molecular information of cellular niches and tissue architecture facilitates greater identification of targetable mechanisms compared to conventional histological and immunofluorescence-based analyses. Neighborhood analysis extends beyond detecting the existence of tissue similarities and differences and instead enables a detailed understanding of cell properties driving spatial neighborhoods and the dynamic molecular interactions within them.<sup>4,67,68</sup> Giotto<sup>69</sup> and Squidpy<sup>70</sup> are two spatial analysis packages with built-in neighborhood analysis tools to evaluate differences in gene or protein expression across heterogeneous tissue architecture. Moreover, numerous groups are developing their own neighborhood analysis algorithms.<sup>71–73</sup> For example, Wu et al. created a spatial cellular graphical model (SPACE-GM) to explore the local arrangement of tumor cell communities in which they identified two tissue architectures that were distinctly spatially arranged and corresponded to different patient outcomes.<sup>72</sup>

Neighborhood analysis can also identify particularly mitogenic and infiltrative regions of a tumor tissue.<sup>74–76</sup> In analyzing spatial transcriptomic data of human H3-K27M

mutant diffuse midline glioma tissue, Liu et al. performed neighborhood analysis to investigate the single-cell spatial organization of these tumors.<sup>77</sup> They identified distinct spatial niches of proliferating tumor cells that resembled oligodendrocyte precursor cells and oligodendrocytes, surrounded by non-proliferating tumor cells that resembled astrocytes, indicating that specific tumor cell subtypes have distinct spatial neighborhoods within the larger heterogeneous tumor. In another study, Hunter et al. used a zebrafish melanoma model and identified regions along the tumor boundary in which malignant cells upregulated cilia genes, suggesting a spatially defined transcriptional neighborhood of mitogenic cells underlying melanoma cell invasion.<sup>78</sup> Neighborhood analysis can also identify architectural patterns, such as spatially variable tissue features like hypoxia or necrosis.<sup>79,80</sup> For example, Greenwald et al. performed spatial neighborhood analysis to uncover the organization of cell states in human glioblastoma (GBM).<sup>79</sup> Starting from the tumor core, they identified five distinct cell state layers: (1) the hypoxic niche, (2) the hypoxia-adjacent niche, (3) the immune and angiogenesis-related niche, (4) the neurodevelopmental GBM state, and finally (5) the normal brain. Their analysis identified hypoxia as a driving factor underlying the layered spatial organization across cancer cell states. Ultimately, both subcellular and community-level investigation into spatially distinct microenvironments explains aspects of tumor heterogeneity and may elucidate new therapeutic approaches.

#### Inference of ligand-receptor interactions mediating tumor progression and treatment resistance

Ligand-receptor interactions play a crucial role in multicellular communication that promotes cancer cell survival, proliferation,

and evasion of immune- and treatment-induced cell death. Ligand-receptor interaction-mediated treatment resistance has been observed in several preclinical and clinical models. For example, most receptor tyrosine kinase (RTK) ligands, such as epidermal growth factor (EGF),<sup>81</sup> vascular endothelial growth factor (VEGF),<sup>82</sup> and insulin-like growth factor (IGF),<sup>83</sup> as well as their respective receptors, are known to be expressed by cancer cells, stromal cells, and other cellular constituents of the TME. When bound, RTK ligands activate pro-survival signaling pathways in response to chemo- and radiotherapy, contributing to treatment resistance. Notably, many ligand-receptor pairs are activated by both autocrine and paracrine signaling, indicating a significant degree of complexity and redundancy that may be poorly captured by dissociative single cell approaches.<sup>84,85</sup> Thus, integrating the spatial position of cells involved in ligand-receptor signaling in the TME with molecular information will enable more precise inference of relevant ligand-receptor interactions and their potential as therapeutic targets.<sup>86–88</sup>

To power ligand receptor interaction analyses, sparse spatial datasets are commonly combined with higher sensitivity scRNA-seq datasets to map single cell profiles in space. For example, to identify ligand-receptor networks present in human cutaneous squamous cell carcinoma, Ji et al. integrated scRNA-seq with spatial transcriptomics data and multiplexed ion beam imaging.<sup>89</sup> Their findings not only revealed a unique subpopulation of resistant and invasive carcinoma cells, but also provided insights into the high degree of ligand-receptor mediated communication with cancer-associated fibroblasts (CAFs) and endothelial cells in the TME. Similarly, Ferri-Borgogno et al. integrated scRNA-seq with spatial transcriptomics and identified relevant ligand-receptor interactions in treatment-resistant high-grade serous ovarian cancer (HGSC), revealing increased APOE-LRP5 signaling between spatially proximal tumor cells and CAFs in the ovarian TME of patients who were short-term survivors compared to long-term survivors.<sup>90</sup>

While these studies inferred ligand-receptor interactions by integrating different -omic approaches, RNA *in situ* hybridization-based imaging methods such as spatial molecular imaging (SMI) enable the identification of ligand-receptor interactions at single-cell resolution in the native tissue context. For example, our group performed SMI of human pancreatic ductal carcinoma (PDAC) to identify ligand-receptor interactions that are altered in response to treatment.<sup>91</sup> We developed SCOTIA (spatially constrained optimal transport interaction analysis) as a computational approach to infer ligand-receptor interactions from single-cell spatial omics by considering both spatial distance and ligand-receptor gene expression between individual cells in the TME.<sup>91</sup>

Advances in computational analysis have created standardized workflows for users to infer ligand-receptor interactions from spatial -omic datasets. For example, SpaOTsc uses optimal transport algorithms to recover relevant spatial measurements of a handful of genes identified using scRNA-seq.<sup>30</sup> Giotto infers ligand-receptor interactions by determining whether two cells are spatially proximal to each other in the tissue, identifying known ligand-receptor binding pairs that are co-expressed, and ranking which ligand-receptor pairs are likely to functionally interact between adjacent cells.<sup>69</sup> COMMOT (communication analysis by optimal transport) infers ligand-re-

ceptor interactions while considering ligand-receptor binding competition present in multicellular tissues.<sup>92</sup> SpatialDM is a statistical model that identifies specific locations (spots) and patterns shared by ligand-receptor pairs to infer their interactions and patterns of broader cell-cell communication.<sup>93</sup> Incorporating these advanced computational analyses of spatial data provides a more comprehensive landscape of clinically relevant ligand-receptor interactions.

### Therapeutic targets at the tumor-stroma interface

#### Cancer-associated fibroblasts

CAFs are stromal cells in the TME of many cancers demonstrated to promote tumor cell proliferation and invasion through various growth and signaling pathways, including the expression and secretion of mitogenic epithelial growth factors, ECM-remodeling proteases, and inhibition of antitumor inflammatory responses.<sup>94–99</sup> CAFs have been demonstrated to promote treatment resistance by creating a supportive and compliant TME.<sup>100</sup> Notably, functionally distinct CAF subtypes exist and while typically associated with peripheral tumors,<sup>101,102</sup> evidence suggests certain CAF subtypes also inhabit brain tumors and are spatially co-enriched with cancer stem cell niches.<sup>103</sup> Applying spatial tools to dissect CAF subtypes and enrichment patterns in tumor tissue is therefore a therapeutic priority.

For example, Peng et al. performed spatial transcriptomics of colorectal cancer patient tissue and classified two distinct types of CAFs in the TME: myofibroblast-associated CAFs (mCAFs) and inflammatory-associated CAFs (iCAFs).<sup>104</sup> Their findings revealed that mCAFs were spatially co-enriched with anti-tumor immune cells while iCAFs were spatially co-enriched with markers of immunosuppression, epithelial-mesenchymal transition (EMT), and lipid metabolism, indicating an interaction in the tumor-stroma microenvironment facilitating cancer cell proliferation and invasion. Additionally, iCAF expression was enriched in the tissue of patients who underwent chemotherapy and associated with lymph node invasion, suggesting a potential mechanism of drug resistance and tumor metastasis.

In the context of non-small cell lung cancer (NSCLC), Cords et al. performed spatially resolved single-cell imaging mass cytometry on human NSCLC tissue and used CAF composition to classify patients into prognostic groups.<sup>105</sup> Their analysis identified spatially and functionally distinct CAF subtypes and found that tumor-like CAFs (tCAFs) and hypoxic tCAFs were enriched in patients diagnosed with distant metastases, in patients who had relapsed after chemotherapy, and in patients who experienced overall shorter survival. Further, they found that tCAFs mediate adenosine production near tumor cells, suggesting a mechanism of CAF-mediated tumor growth. In another study, Zhang et al. performed spatial transcriptomics to investigate differences in the TME of hepatocellular carcinoma (HCC) among patients who responded and did not respond to combination therapy (anti-VEGF and immune checkpoint inhibitor).<sup>106</sup> Their analysis indicated that the TME of patient tumors that responded to treatment were enriched with immune cells and CAFs expressing proinflammatory signals. In contrast, non-responder tumors were depleted of immune cells but were instead enriched with a distinct CAF subtype and expressed key metabolic, cancer stem cell, and immune evasion genes.<sup>106</sup> Collectively, these studies provide contextual information

regarding the spatial distribution of cellular niches within heterogeneous tissue, such as CAF organization, demonstrating the utility of spatial context for identifying targetable interactions to disrupt CAF signaling in the TME.

### Tumor-immune interactions

While there has been a surge in the development and use of immunotherapies, such as immune-checkpoint inhibitors, immune-based vaccines, and adoptive cell therapy, the effectiveness of these approaches varies by cancer and patient.<sup>107</sup> Immune infiltration into the local TME is often characterized as a pro-inflammatory phenotype in which various immune cells accumulate around and within the tumor. In reality, this process can result in anti- or pro-tumor effects depending on the types and states of the infiltrating immune cells. It is thus critical to gain a deeper understanding of the complex interactions between tumor and immune cells to determine how to best enhance anti-tumor and inhibit pro-tumor phenotypes.

Hirz et al. employed spatial transcriptomics to characterize the immune suppressive TME of human prostate tumors to further understand targetable tumor-immune cell interactions.<sup>108</sup> Their findings revealed that primary prostate cancer establishes a largely suppressive immune microenvironment due to a spatially localized accumulation of myeloid-derived suppressor cells in combination with low T cell infiltrate, signifying exhausted T-cells. Further analysis revealed that stromal cells and tumor cells expressed high levels of chemokines involved in myeloid differentiation and recruitment via ligand-receptor interactions, indicating bidirectional communication between spatially proximal cells to support tumor growth and progression, consistent with other studies in the field.<sup>109</sup> Interestingly, they also found monocyte subpopulations within the immunosuppressive prostate TME to demonstrate significant spatial enrichment with angiogenic and metastatic factors, suggesting other possible mechanisms underlying immune cell-mediated tumor growth and invasion.

Studies have also investigated tumor-immune interactions of specific tumor types that demonstrate unpredictable responses to immunotherapies, such as GBM, which is known to be highly resistant due to its immunosuppressive TME.<sup>110-112</sup> Ravi et al. applied integrative multidimensional modeling of single cell and spatially resolved gene expression data of immune cells from patient GBM tissue to investigate the tumor-infiltrating lymphoid compartment.<sup>112</sup> Their results suggest that T cell exhaustion in GBM was driven by myeloid cell-mediated IL-10 signaling. They also found that these tumor-associated myeloid cells were localized with mesenchymal-like tumor cells, which are known to engage in tumor-immune crosstalk and contribute to an immunosuppressive GBM microenvironment. Continued investigation into tumor-immune interactions in the TME will highlight vulnerabilities that can be therapeutically targeted.

### Tumor-nerve interactions

The emerging field of cancer neuroscience has greatly advanced our understanding of the reciprocal interactions between tumors and nerves in the TME and has demonstrated the need to consider the central and peripheral nervous systems (CNS and PNS) as active regulators of cancer development, progression, and metastasis.<sup>113</sup> For example, in peripheral tumors such as pancreatic and prostate cancer, perineural invasion (PNI), or the invasion of cancer cells into and around nerves, is associated

with an increased incidence of tumor recurrence and metastasis leading to poor patient outcomes.<sup>114</sup> Investigating tumor-nerve interactions may lead to the development of neuromodulatory cancer therapies to both inhibit tumor growth and improve the management of cancer-related pain and neuronal dysfunction.

To investigate the significance of tumor-nerve interactions in the context of human oral squamous cell carcinoma (OSCC), Schmid et al. performed spatial transcriptomic profiling of PNI-positive and PNI-negative nerves in malignant and nonmalignant surrounding tissue.<sup>115</sup> Their analysis indicated that nerves spatially proximal to cancer cells upregulate genes associated with injury and stress responses, as well as genes associated with neurite growth, axonogenesis, and regeneration. They suggest that tumor-mediated nerve injury results in a regenerative nerve response that manifests in a spatially gradient expression pattern and may influence tumor behavior. Importantly, their findings reveal that tumor-nerve distances predict patient survival, such that closer tumor-nerve distances result in poorer survival and that large nerve(s) in malignant tissue regions are also associated with worse patient survival.

In a multi-omic study of human GBM, Ravi et al. investigated the impact of the neuronal brain environment in altering the spatial presentation of transcriptional, metabolic, and proteomic programs present in GBM.<sup>116</sup> Their spatial analysis revealed several spatially distinct transcriptional and metabolic programs that arise in cancer cells in response to inflammation, metabolic stimuli, or general cell stress within the neuronal environment, similar to the reactive response of glial cells in response to specific neural signals. While precise mechanisms of tumor-nerve interactions are still an active area of research, these interactions are recognized as potential therapeutic targets.

## SPATIAL BIOMARKERS

In this section, we discuss biomarkers identified through spatial omics that are prognostic of clinical outcomes or predictive of response to therapy, highlighting the translational promise of spatial biology. Although many steps remain before these pre-clinical findings can be integrated into clinical practice, these early examples of spatial biomarkers demonstrate immense promise ultimately be impactful in both preclinical discovery and clinical management.

### Predicting response to immunotherapy

Studies in spatial biology have revealed spatially organized immunological features and cell states related to prognosis and treatment response to immunotherapies.<sup>117-120</sup> Allam et al. used multiplexed markers on lung tumor samples to develop SpatialVizScore,<sup>118</sup> which characterizes immune cell state and quantifies infiltration level, identifying three major categories of immune infiltration: immune-inflamed, immune-suppressed, and immune-cold. While immune-suppressed tumors may show moderate to high infiltration of immune cells, this includes abundant M2-polarized, PD-L1 expressing tumor associated macrophages (TAMs) that promote an immunosuppressive environment. Samples with high levels of CD8<sup>+</sup> T cell infiltration levels had heterogeneous correlation with macrophage polarization or other modifiers of the immune milieu, demonstrating that the complexity of the immune microenvironment may be better

captured with this higher-dimensional scoring system. Similarly, in human PDAC samples, while there was no correlation between leukocyte infiltration levels and survival, a risk score derived from the relative distances from IL10<sup>+</sup> myelomonocytes to PD-1<sup>+</sup> CD4<sup>+</sup> T cells and GZMB<sup>+</sup> CD8<sup>+</sup> T cells was predictive of survival.<sup>119</sup> Finally, Phillips et al. developed a *SpatialScore* in cutaneous T cell lymphoma based on the physical distance ratio of each CD4<sup>+</sup> T cell and its nearest cancer cell relative to its nearest Treg such that a lower *SpatialScore* is indicative of higher T cell effector activity and a higher *SpatialScore* is suggestive of increased T cell suppression.<sup>117</sup> Indeed, the *SpatialScore* biomarker was able to predict patient response to pembrolizumab while conventional biomarkers utilizing IHC, gene expression profiling, and mass cytometry did not predict therapeutic response.<sup>121</sup> Thus, more complex scores derived from spatial transcriptomics may better prognosticate clinical outcomes and predict response to immunotherapies.

Other studies have similarly demonstrated that macrophage subsets are critical to predict clinical outcomes. In GBM, macrophage infiltration has been associated with higher tumor grade and spatial proteomic data revealed that cellular neighborhoods enriched for M1-polarized macrophages and a neutrophil-like MPO<sup>+</sup> macrophage subtype were correlated with long-term survival.<sup>122</sup> This provides a potential explanation as to why CSF-1R inhibitors that broadly target and deplete all macrophage subsets have had only modest efficacy. High-plex spatial studies have also highlighted other subsets of macrophages that correlate with outcomes in cancer.<sup>123–125</sup> For example, CODEX studies in breast and colorectal cancer discovered that FOLFR+ TAMs colocalize with plasma cells and are associated with better survival, while SPP1+ TAMs are found in hypoxic and necrotic tumor areas and are associated with worse clinical outcomes.<sup>125</sup>

Patients receiving ICB are now routinely assessed for IHC expression of the relevant immune checkpoint protein(s) via measures like the total positive score (TPS) or combined positive score (CPS) that determine eligibility for anti-PDL1 therapy.<sup>126</sup> However, individual tissue-based biomarkers are not always well-correlated to immunotherapy response; indeed, recent studies have shown that gene expression-based scores may be more predictive of response to anti-PDL1 therapy compared to PDL1 IHC or tumor mutational burden.<sup>127–129</sup> One such score, the immunotherapy response score (IRS), which integrates tumor mutational burden and TPS/CPS with the expression of four target genes (CD274, PDCD1, TOP2A, and ADAM12), improved prediction of progression free survival across 23 tumor types.<sup>128</sup> High-resolution spatial tools that localize gene expression to specific cellular compartments have further highlighted that the specific location of gene expression modifies the efficacy of immune checkpoint inhibitors. For example, in triple-negative breast cancer, intraepithelial PD-L1 RNA expression is correlated with increased recurrence free survival and an inflammatory milieu, while PD-L1 expression on macrophages in the peritumoral stroma is correlated with worse prognosis and T-regulatory cell infiltration, promoting disease progression.<sup>130,131</sup> On the other hand, in melanoma, PD-L1 expressed specifically on macrophages and not the tumor cells, was associated with increased overall survival.<sup>132</sup> These studies highlight the limitations of using broad markers that are not cell-type spe-

cific to determine eligibility for immunotherapy and highlight the importance cell type-specific targeting for drug development. With the generation of spatial profiling datasets across diverse cancer types, the development of refined cell-type specific transcriptional signatures to predict immunotherapy response is within reach.

### Spatial organization of immune cells as biomarkers of prognosis and treatment response

Additionally, spatial biology highlights architectural organization in tissue—particularly of immune cells—that show promise as biomarkers of prognosis and treatment response.<sup>119,133–136</sup> In particular, tertiary lymphoid structures (TLS) have emerged as structural components of the TME that indicate better prognosis<sup>137</sup> and response to immunotherapy.<sup>138</sup> TLS are ectopic lymphoid aggregates that form in sites of persistent inflammatory stimulation to support a local immune response. Identifying TLS has historically been labor-intensive and required a trained pathologist to identify.<sup>74,137</sup> This is in part due to heterogeneity of TLS across patients and that even if TLS exist in a cancer specimen, they may not be fully captured in the specific sections under examination. Importantly, spatial transcriptomics provides better characterization of lymphoid structures in that one can better differentiate between small lymphoid aggregates and TLS despite limited sampling by identifying differentiating expression patterns. Andersson et al. used spatial transcriptomics in HER2+ breast cancer to create an expression-based signature for TLS based on the colocalization of B and T cells. This signature contained genes not only relate to T and B cells (e.g., MS4A1, B2M, and TRBC2), but also homing genes (CXCL13 and CXCR5) and other genes associated with TLSs, that was predictive of overall survival when applied to bulk RNA-seq datasets from cutaneous melanoma.<sup>137</sup> Identifying such a signature in bulk or dissociated single-cell transcriptomic data would be impossible due to infrequency in the TME and lack of knowledge of spatial organization, respectively, making it difficult to differentiate between an organized TLS structure versus infiltrating immune cells. However, the resolution of spatial profiling allows the derivation of a transcriptomic signature of this spatial biomarker with prognostic value. This highlights the translational potential of these spatial biomarkers in clinical workflows, as application of transcriptional signatures derived from spatial experiments can then be adapted to an accessible assay such as bulk transcriptomics. This approach may enable the identification of patients who are likely to have TLS that may not be obvious in specific tissue sections.

In addition to helping to identify TLS and other immunity hubs, studies in spatial biology have also enabled an understanding of the underlying biology maintaining these structures.<sup>133,138,139</sup> For example, in renal cell carcinoma, Meylan et al. found that plasma cells in TLS migrate toward the tumor along fibroblast tracks that secrete CXCL12.<sup>138</sup> In colon cancer, Pelka et al. identified hubs of CXCL10/CXCL11<sup>+</sup> malignant and myeloid cells colocalized with IFNG<sup>+</sup>/CXCL13<sup>+</sup> T cells, suggesting a positive feedback loop wherein T cell-derived IFN $\gamma$  induces expression of CXCR3 ligands from malignant and myeloid cells, which in turn attracts more T cells to the local microenvironment.<sup>133</sup> Together, these studies uncover pathways that can be targeted

to impact the organization of immune cells and promote anti-tumor immunity.

A recent study revealed that heterogeneity in antibody producing cells also impacts antitumor immunity across multiple cancer types.<sup>140</sup> Different cancer types showed distinct compositions of B cell states. For example, germinal center B cells were abundant in colorectal cancer, inducing TLS with mature GC structure; conversely, in HCC and pancreatic ductal adenocarcinoma the alternative extrafollicular pathway predominated, leading to an exhausted atypical memory (AtM) B cell phenotype and formation of immature TLS. Analysis of spatial transcriptomic data across multiple cancer types showed that AtM B cells spatially colocalized with PD1<sup>+</sup>CXCL13<sup>+</sup>CXCR5<sup>-</sup> peripheral T helper cells in TLS. Co-culture experiments showed that Tph cells induced differentiation of B cells into AtM cells and conversely that AtM B cells promoted the differentiation of T cells into T-reg and exhausted T cells. The presence of AtM B cells was associated with worse clinical prognosis across multiple cancer types and correlated with treatment resistance to anti-PD1 therapy. These results show that functional immune cell subsets within TLS can dramatically impact the anti-tumor immune response, highlighting the importance of spatial profiling to studying the complexity and heterogeneity of TLS composition across cancer types.

### Identification of the tumor invasive front

Spatial biology has also helped to identify and characterize cellular interactions at the TIF. TIF describes the niche of malignant cells in the outermost ring of tumor that interacts with surrounding nonmalignant cells. Studying cellular interactions at the TIF has elucidated mechanisms of tumor invasion and adaptation to different environments.<sup>74,141–144</sup> In particular, malignant cells in the TIF express genes related to EMT and are surrounded by an immunosuppressive microenvironment.<sup>74,142,143,145</sup> In liver cancer, malignant cells maintain this immunosuppressive environment through TIF malignant cells expressing CXCL6, which induces the overexpression of serum amyloid A proteins (SAA) in nearby damaged hepatocytes, resulting in the recruitment and polarization of M2 macrophages.<sup>142</sup> Further, this community of hepatocytes overexpressing SAA at the tumor border is associated with worse prognosis. By integrating spatial metabolomics Liu et al. found that malignant cells at the TIF in breast cancer upregulate the oxidative phosphorylation pathway in early dissemination, suggesting that this pathway plays a role in the early metastatic process.<sup>144</sup> Furthermore, the expression of genes related to oxidative phosphorylation was associated with worse overall survival and distant metastasis-free survival when applied to scRNA-seq datasets of breast cancer. Thus, not only are gene expression programs expressed at the TIF informative of mechanisms of invasion, but also can be prognostic.

Historically, defining the TIF has been subjective, based on IHC staining without clear criteria or consistent methods. However, spatially resolved transcriptomic data have enabled the identification of gene expression regions and inference of copy number variants that can distinguish malignant from nonmalignant regions.<sup>143,146,147</sup> Berglund et al. performed spatial transcriptomics in prostate cancer to reveal differences in gene expression between the cancer core and surrounding stroma.<sup>146</sup> Furthermore, their study revealed that the gene expression pro-

file of malignant cells extended to regions beyond the boundaries of pathologist-annotated tumor areas. Similarly, in human OSCC, Arora et al. revealed that TIF malignant cells were enriched for genes related to cell cycle, EMT, and angiogenesis.<sup>143</sup> When applying this leading-edge transcriptional signature to tumors from other tissue types, they found that this signature was associated with worse clinical outcomes. Using these transcriptomic-based tools to identify the TIF could improve delineation of the TIF, helping to identify patients who may still have invasive disease.

### CLINICAL INTEGRATION

#### The ideal clinical spatial platform

For spatial analyses to be useful for clinical decision-making, the platform in question should meet several criteria. First, the instrument should be compatible with sample preparations utilized in clinical pathology workflows, namely FFPE specimens or fresh-frozen sections. The second criterion is ease of use. Each spatial platform will have different reagent and instrumentation requirements, with some involving customized slides and others needing advanced imaging equipment that may not be as feasible for widespread clinical adoption. Therefore, a clinically desirable platform would be one that can incorporate workflows that are already widely implemented in the clinic. Throughput is another criterion that is critically important if labs are to fully integrate spatial profiling into everyday clinical care. Currently, hands-on experimental procedures and automated imaging and processing can take weeks for high-plex imaging-based platforms, which limit their clinical utility. The fourth criterion is plex and resolution. The ideal spatial platform would be one that can flexibly exploit both extremes of plex and resolution to address a variety of clinical objectives. For clinical use, low-plex assays may be ideal to meet throughput demands whereas higher-plex assays with lower throughput can be optimal for discovery-based research. Cost is a final criterion and can include both total instrument cost and cost per analyte for a given sample. Proteomic approaches, which employ antibodies for spatial profiling, will have higher cost per analyte than transcriptomic approaches. However, even for transcriptome profiling, costs can still reach up to thousands of dollars per slide. Reduction in cost is critical if spatial platforms are to be affordable for clinical use.

#### Moving toward clinical deployment of spatial oncology

Compared to dissociative omics approaches that are commonplace in the research laboratory, spatial profiling is uniquely suited to integrate into clinical workflows. Clinicians are accustomed to routine review of histopathological images and findings during multidisciplinary tumor boards. Spatial profiling thus confers a natural and intuitive extension of existing tissue analyses, such as H&E, that are performed routinely in the clinic. To maximize the clinical utility of spatial profiling, pathologists and bioinformaticians will be essential for spatial decision-making. A routine clinical spatial workflow could involve sectioning a tumor sample into two slides and sending one slide for H&E staining and the other for spatial analysis. A skilled pathologist would be able to offer authoritative insight pertaining to tissue annotation, cell type identification, assessment of tumor grade, etc. on

H&E samples that can in turn better inform the planning of corresponding spatial analyses. Spatial technologies that are imaging-based, especially, require the selection of regions of interest (ROIs) or fields of view (FOVs) prior to acquisition; therefore, input from pathologists can ensure that ROIs/FOVs are optimally placed to balance comprehensive profiling with instrument run time.

### Standardization of spatial workflows for clinical use

Before any spatial profiling approaches are brought to the clinic, there needs to be prior optimization and standardization of a workflow that has undergone rigorous validation of target analytes. Collaborations across multiple institutions may be beneficial for such validation efforts to ensure reproducibility and accuracy across clinical teams. For example, six laboratories previously led a multi-institutional effort to validate a six-plex (PD-L1, PD-1, CD8, CD68, FOXP3, and CK) mIF workflow for characterization of the PD-1/PD-L1 axis.<sup>148</sup> All six locations were able to achieve intra- and inter-site reproducibility of the mIF procedure that included automated staining, multispectral imaging, and machine learning-trained image analysis, effectively setting forward a framework for assessing reproducibility of future mIF panels for spatial proteomics.<sup>148</sup> Ideally, protein and RNA probes will need to be individually titrated and optimized in a tissue-specific manner. Existing platforms such as AstroPath have also laid out generalizable frameworks for improving imaging and data collection steps in spatial workflows which can assist with standardization and cross-site/study comparisons.<sup>149</sup> Developing standardized protocols for more upstream procedures such as sample preparation and tissue processing will also be crucial for generating high-quality spatial data. Liu et al., for instance, emphasize the importance of standardizing temporary preservation conditions in the operating room (OR), freezing approaches, storage duration of frozen samples, and transportation from OR to laboratory in a way that minimizes sample exposure to room temperature.<sup>150</sup> Transcriptomic approaches, especially in the context of FFPE samples, will require additional attention to variables such as formalin fixation time and age of blocks to most fully preserve the integrity of RNA and minimize analyte degradation or modification.<sup>151,152</sup> Therefore, standardizing end-to-end spatial workflows and validating them through preclinical studies and clinical trials will be essential for implementation into the clinic.

### FUTURE PERSPECTIVES

The promise of increasing molecular plex and spatial resolution has a history of lofty expectations yet, in practice, the challenges of clinical integration remain formidable. Single cell sequencing, which has also been used to analyze clinical samples and in many applications serves as a predicate for spatial *in situ* technologies, has yet to find an application in the routine clinical care of patients.<sup>153</sup> It is tempting to speculate that as the sensitivity, throughput, and logistical hurdles relating to data acquisition and storage pertaining to spatial technologies are solved over the coming years, increasingly routine clinical use of such assays has the potential to become widespread. However, prospective clinical validation studies, clinical utility studies, and regulatory benchmarking will likely become the bottleneck for

adaptation of spatial *in situ* technologies, just as they have for simpler diagnostic and prognostic assays. Nevertheless, the frontier of what spatial technologies have the potential to bring to clinical decision making brings exciting possibilities.

Efforts to broaden the scale of spatial analyses in more dimensions beyond the 2D spatial sections that are currently analyzed provide additional opportunities to refine our understanding of the spatial organization of cancer. Beyond spatial analysis of an isolated tumor, organism scale spatial analysis provided by recent tissue clearance protocols will enable in depth study of metastasis in preclinical models.<sup>154</sup> These technologies have already enabled study of organ specific metastatic tropism, routes of dissemination, and pharmacologic treatments aimed at reducing metastatic burden. Serial sectioning of tissue specimens have also been used to generate high resolution 3D maps of tumors with computational reconstruction of H&E staining on consecutive sections.<sup>155,156</sup> These techniques will help answer questions related to tumor evolution and resolve features that are poorly captured by thin 2D sections.

Another exciting area of future development for spatial technologies is expanding analysis to explore gene expression changes simultaneously over space and time. Spatially resolved genomic and transcriptomic data provide insight into clonal architecture and tumor evolution, highlighting differences in micro-environment composition.<sup>68,157–160</sup> For example, BaSSIS provides spatially resolved genomic and transcriptomic data from serial sections by creating targeted probes against subclonal mutations, which was used to demonstrate that breast cancer subclones have distinct tumor microenvironments.<sup>158</sup> Computational techniques to infer changes in gene expression across time with RNA velocity and pseudotime analyses have been well established in scRNA-seq analyses.<sup>161–163</sup> However, tools to apply this analysis to spatial transcriptomics that fully utilize spatial dimensionality, such as stLearn, are emerging and promising to examine changes in gene expression across progression from precancerous to cancerous lesions and across tumor subclones.<sup>164</sup> Finally, to combat the inherent challenge that tissue sections are a static “snapshot-in-time,” emerging technologies enable the mapping of live cells through space and time in both *in vitro* and *in vivo* model systems.<sup>165,166</sup> For example, Raman2RNA imputes single-cell transcriptional profiles from live-cell, label-free Raman scattering microscopy in *in vitro* systems.<sup>166</sup> As Raman microscopy has also been used for intraoperative genetic profiling of GBM<sup>167</sup> and on FFPE sections to maintain spatial context,<sup>168</sup> one could imagine using it to also profile transcriptional and metabolomic profiles of patient samples in real time to guide clinical decision making.

An emerging field has focused on biomarker and gene expression prediction directly from routine H&E staining using artificial intelligence (AI) approaches. Tumor morphological features and spatial organization patterns can in some instances directly be used as biomarkers in lieu of more complex alternatives that require special stains or IHC. For example, whole slide H&E images can be used to predict origins for cancers of unknown primary using deep learning,<sup>169</sup> addressing an important clinical scenario that impacts treatment decision making. Integrating these tools with existing digital pathology workflows provides an avenue for clinical use in existing workflows. Further prospective studies and regulatory approval of such tools could provide

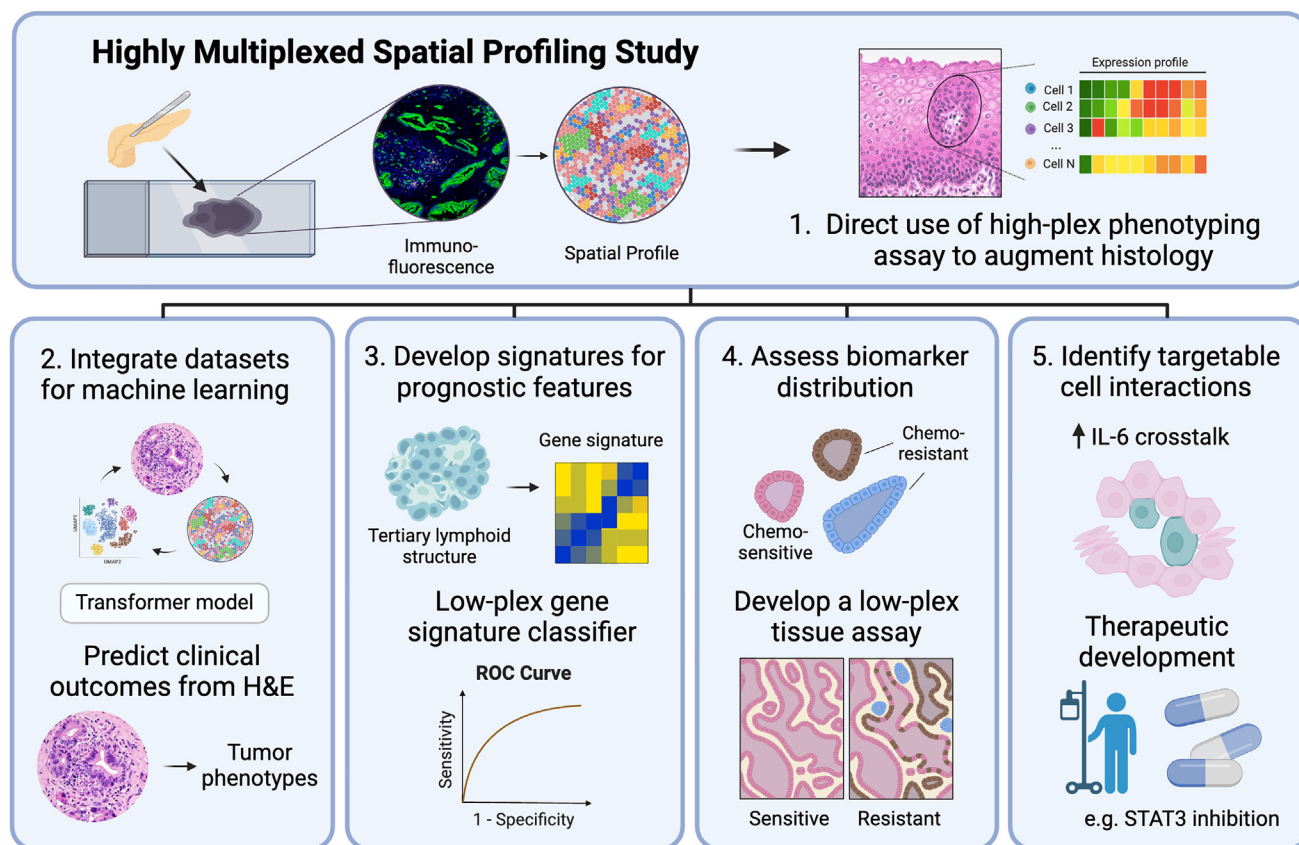


Figure 3. Clinical applications of spatial profiling

broad clinical utility with cost and time savings. As spatially resolved -omics datasets grow in size and abundance, advanced machine learning models have also been trained to infer gene expression both at a bulk level and single cell profiles from H&E slides.<sup>170,171</sup> AI models trained on H&E slides with paired bulk transcriptomic data are able to predict common oncogene mutations, transcriptional subtypes, and prognostic information.<sup>172–174</sup> In the future, machine learning models capable of utilizing multi-omic inputs including H&E images, bulk transcriptome measurements, genomic profiling, and clinical history could further improve prediction of clinically relevant metrics including treatment response, disease recurrence, and prognosis.

Importantly, the eventual translation of spatial profiling technologies into clinical use does not necessarily require direct use of highly multiplexed spatial profiling on clinical specimens (Figure 3). Rather, the benefits of spatial profiling may be more economically realized by low-pex assays that have already demonstrated widespread use and clinical utility. For example, highly multiplexed spatial profiling can be used to identify a focused panel of biomarkers that capture the biological signal. The ACR-368 OncoSignature is the first example of a companion diagnostic receiving an FDA Breakthrough Device designation to use a small PhenoCycler multiplexed protein imaging panel to select patients that may benefit from treatment with ACR-368. Similarly, spatial profiling tools may sift through the high-pex

data to distill the minimal set of genes that can reliably predict the phenotype of interest that can then be implemented through more economical bulk transcriptomics or IHC methods.<sup>175</sup> Machine learning models trained on paired spatial profiling and H&E stained sections could be directly integrated into digital pathology workflows to augment pathological review with molecular information, such as to identify TLS or the TIF.<sup>176</sup> Similar to how genomically guided companion diagnostics measure gene expression or genetic alterations to predict response to treatment, highly multiplexed profiling of cell surface antigens on clinical specimens may provide an analogous companion diagnostic tool for antibody drug conjugates, chimeric antigen receptor T cells, or other antigen directed therapies. While the use of spatial profiling technologies to identify new drug targets is still in its infancy, highly multiplexed spatial analysis of the TME could contribute to drug development and clinical trial workflows by characterizing emergent cell-cell interactions involved in cancer progression and mechanisms of therapeutic resistance.

Finally, recent efforts have attempted to clarify the added benefits of leveraging deeper characterization of patient samples to solve challenges in drug development and clinical management; however, there remains a fundamental statistical challenge when using large scale datasets. By themselves, they are limited by the fact that deep characterization creates a multiple comparisons problem where biological inferences can be limited in statistical power when in theory each patient's tumor is unique. However,

the recent development of human tissue atlasing projects through organizations and efforts including The Human Cell Atlas,<sup>177</sup> the NCI's Human Tumor Atlas Network<sup>178</sup> (HTAN), the Human BioMolecular Atlas Program (HuBMAP), and the Multi-Omic Spatial Atlas in Cancer<sup>179</sup> (MOSAIC) project have provided the means to integrate and query any given patient's tumor profile against existing datasets of previously profiled tumors. Continuous integration and reference mapping of clinical samples to reach biobank scale single cell and spatial datasets,<sup>180,181</sup> could lead to the emergence of new insights. Conquering the heterogeneity of cancer ecosystems through scale will inevitably be an expensive and time-consuming endeavor but may be the optimal way to contextualize any patient's tumor within our collective understanding of the disease.

## CONCLUSIONS

*In situ* spatial profiling technologies are a breakthrough class of methods that have already redefined how cancer biology research is performed. The continued development and application of these technologies will enable biological phenomena to be placed in their native tissue context and allow researchers to observe the emergent properties involved in cancer progression. Spatial resolution will enable inference of cell-cell interactions and lead to the design of new therapeutic strategies targeting the TME. Like any new class of assays, these technologies now face the challenge of proving robust clinical utility in prospective studies and making technical improvements that guarantee consistent high quality and interpretable data. Additionally, infrastructure to support the integration of these technologies into clinical research including secure platforms for data storage, easy to interpret pipelines for data analysis, and standardization of assay protocols will play a critical role in broader adoption. Overall, we are optimistic that these novel technologies will play a significant role in identifying new strategies for therapeutic intervention and identifying novel spatial biomarkers to shape precision oncology for many years to come.

## ACKNOWLEDGMENTS

This work was supported in part by an NSF Graduate Research Fellowship Program (D.G.), NCI K08CA270417 (W.L.H.), Burroughs Wellcome Fund Career Award for Medical Scientists (W.L.H.), Pancreatic Cancer Action Network Career Development Award (W.L.H.), and Krantz Family Center for Cancer Research Quantum Award (W.L.H.). The funders had no role in the manuscript.

## DECLARATION OF INTERESTS

W.L.H. has received grant funding from Akoya Biosciences and conference travel reimbursements from Nanostring Technologies related to spatial oncology studies. W.L.H. is an inventor on U.S. Provisional Patent Application No. 63/069,035 and No. 63/346,670, as well as International Patent Application No. PCT/US2021/047041 and No. PCT/US2023/067607.

## REFERENCES

- Haggard, H.W., and Smith, G.M. (1938). Johannes Müller and the Modern Conception of Cancer. *Yale J. Biol. Med.* **10**, b1–b436.
- Walsh, L.A., and Quail, D.F. (2023). Decoding the tumor microenvironment with spatial technologies. *Nat. Immunol.* **24**, 1982–1993. <https://doi.org/10.1038/s41590-023-01678-9>.
- Klemm, F., Maas, R.R., Bowman, R.L., Kornete, M., Soukup, K., Nassiri, S., Brouland, J.-P., Iacobuzio-Donahue, C.A., Brennan, C., Tabar, V., et al. (2020). Interrogation of the Microenvironmental Landscape in Brain Tumors Reveals Disease-Specific Alterations of Immune Cells. *Cell* **181**, 1643–1660.e17. <https://doi.org/10.1016/j.cell.2020.05.007>.
- Seferbekova, Z., Lomakin, A., Yates, L.R., and Gerstung, M. (2023). Spatial biology of cancer evolution. *Nat. Rev. Genet.* **24**, 295–313. <https://doi.org/10.1038/s41576-022-00553-x>.
- Gibbs, S.N., Peneva, D., Cuyun Carter, G., Palomares, M.R., Thakkar, S., Hall, D.W., Dalgliesh, H., Campos, C., and Yermilov, I. (2023). Comprehensive Review on the Clinical Impact of Next-Generation Sequencing Tests for the Management of Advanced Cancer. *JCO Precis. Oncol.* **7**, e2200715. <https://doi.org/10.1200/PO.22.00715>.
- Pourmaleki, M., Socci, N.D., Hollmann, T.J., and Mellinghoff, I.K. (2023). Moving Spatially Resolved Multiplexed Protein Profiling toward Clinical Oncology. *Cancer Discov.* **13**, 824–828. <https://doi.org/10.1158/2159-8290.CD-22-1015>.
- Pisapia, P., L'Imperio, V., Galuppini, F., Sajjadi, E., Russo, A., Cerbelli, B., Fraggetta, F., d'Amati, G., Troncone, G., Fassan, M., et al. (2022). The evolving landscape of anatomic pathology. *Crit. Rev. Oncol. Hematol.* **178**, 103776. <https://doi.org/10.1016/j.critrevonc.2022.103776>.
- Vranic, S., and Gatalica, Z. (2023). PD-L1 testing by immunohistochemistry in immuno-oncology. *Biomol. Biomed.* **23**, 15–25. <https://doi.org/10.17305/bjms.2022.7953>.
- Dilawari, A., Shah, M., Ison, G., Gittleman, H., Fiero, M.H., Shah, A., Hamed, S.S., Qiu, J., Yu, J., Manheng, W., et al. (2023). FDA Approval Summary: Mirvetuximab Soravtansine-Gynx for FR $\alpha$ -Positive, Platinum-Resistant Ovarian Cancer. *Clin. Cancer Res.* **29**, 3835–3840. <https://doi.org/10.1158/1078-0432.CCR-23-0991>.
- Vikas, P., Messersmith, H., Compton, C., Sholl, L., Broaddus, R.R., Davis, A., Estevez-Diz, M., Garje, R., Konstantinopoulos, P.A., Leiser, A., et al. (2023). Mismatch Repair and Microsatellite Instability Testing for Immune Checkpoint Inhibitor Therapy: ASCO Endorsement of College of American Pathologists Guideline. *J. Clin. Oncol.* **41**, 1943–1948. <https://doi.org/10.1200/JCO.22.02462>.
- Aman, N.A., Doukoure, B., Koffi, K.D., Kou, B.S., Traore, Z.C., Kouyate, M., Toure, I., and Effi, A.B. (2019). Immunohistochemical Evaluation of Ki-67 and Comparison with Clinicopathologic Factors in Breast Carcinomas. *Asian Pac. J. Cancer Prev. APJCP* **20**, 73–79. <https://doi.org/10.31557/APJCP.2019.20.1.73>.
- Gunderson, C.C., and Moore, K.N. (2015). BRACAnalysis CDx as a companion diagnostic tool for Lynparza. *Expert Rev. Mol. Diagn.* **15**, 1111–1116. <https://doi.org/10.1586/14737159.2015.1078238>.
- Milbury, C.A., Creeden, J., Yip, W.-K., Smith, D.L., Pattani, V., Maxwell, K., Sawchyn, B., Gjoerup, O., Meng, W., Skoletsky, J., et al. (2022). Clinical and analytical validation of FoundationOne®CDx, a comprehensive genomic profiling assay for solid tumors. *PLoS One* **17**, e0264138. <https://doi.org/10.1371/journal.pone.0264138>.
- Haan, J.C., Bhaskaran, R., Ellappalayam, A., Biji, Y., Griffioen, C.J., Lujanovic, E., Audeh, W.M., Penault-Llorca, F., Mittempergher, L., and Glas, A.M. (2022). MammaPrint and BluePrint comprehensively capture the cancer hallmarks in early-stage breast cancer patients. *Genes Chromosomes Cancer* **61**, 148–160. <https://doi.org/10.1002/gcc.23014>.
- Dubsky, P., Brase, J.C., Jakesz, R., Rudas, M., Singer, C.F., Greil, R., Dietze, O., Luisser, I., Klug, E., Sedivy, R., et al. (2013). The EndoPredict score provides prognostic information on late distant metastases in ER+/HER2- breast cancer patients. *Br. J. Cancer* **109**, 2959–2964. <https://doi.org/10.1038/bjc.2013.671>.
- Wallden, B., Storhoff, J., Nielsen, T., Dowidar, N., Schaper, C., Ferree, S., Liu, S., Leung, S., Geiss, G., Snider, J., et al. (2015). Development and verification of the PAM50-based Prosigna breast cancer gene signature assay. *BMC Med. Genom.* **8**, 54. <https://doi.org/10.1186/s12920-015-0129-6>.
- Bagaev, A., Kotlov, N., Nomie, K., Svekolkin, V., Gafurov, A., Isaeva, O., Osokin, N., Kozlov, I., Frenkel, F., Gancharova, O., et al. (2021). Conserved pan-cancer microenvironment subtypes predict response to immunotherapy. *Cancer Cell* **39**, 845–865.e7. <https://doi.org/10.1016/j.ccr.2021.04.014>.

18. Kalinsky, K., Barlow, W.E., Gralow, J.R., Meric-Bernstam, F., Albain, K.S., Hayes, D.F., Lin, N.U., Perez, E.A., Goldstein, L.J., Chia, S.K.L., et al. (2021). 21-Gene Assay to Inform Chemotherapy Benefit in Node-Positive Breast Cancer. *N. Engl. J. Med.* 385, 2336–2347. <https://doi.org/10.1056/NEJMoa2108873>.
19. Carter, P., Alfrangis, C., Cereser, B., Chandrasinghe, P., Belluz, L.D.B., Herzog, T., Levitan, J., Moderau, N., Schwartzberg, L., Tabassum, N., et al. (2018). Does molecular profiling of tumors using the Caris molecular intelligence platform improve outcomes for cancer patients? *Oncotarget* 9, 9456–9467. <https://doi.org/10.18632/oncotarget.24258>.
20. Beaubier, N., Bontrager, M., Huether, R., Igartua, C., Lau, D., Tell, R., Bobe, A.M., Bush, S., Chang, A.L., Hoskinson, D.C., et al. (2019). Integrated genomic profiling expands clinical options for patients with cancer. *Nat. Biotechnol.* 37, 1351–1360. <https://doi.org/10.1038/s41587-019-0259-z>.
21. Wenric, S., Davison, J.M., Wang, Y.E., Mayhew, G.M., Beebe, K., Kang, H.P., Milburn, M.V., Chung, V., Bekaii-Saab, T., and Perou, C.M. (2022). Abstract A002: Purity Independent Subtyping of Tumor (PurlST): Real-world data validation of a pancreatic ductal adenocarcinoma (PDAC) gene expression classifier and its prognostic implications. *Cancer Res.* 82, A002. <https://doi.org/10.1158/1538-7445.PANCA22-A002>.
22. Alix-Panabières, C., and Pantel, K. (2021). Liquid Biopsy: From Discovery to Clinical Application. *Cancer Discov.* 11, 858–873. <https://doi.org/10.1158/2159-8290.CD-20-1311>.
23. Chung, D.C., Gray, D.M., Singh, H., Issaka, R.B., Raymond, V.M., Eagle, C., Hu, S., Chudova, D.I., Talasaz, A., Greenson, J.K., et al. (2024). A Cell-free DNA Blood-Based Test for Colorectal Cancer Screening. *N. Engl. J. Med.* 390, 973–983. <https://doi.org/10.1056/NEJMoa2304714>.
24. Im, Y., and Kim, Y. (2023). A Comprehensive Overview of RNA Deconvolution Methods and Their Application. *Mol. Cell.* 46, 99–105. <https://doi.org/10.14348/molcells.2023.2178>.
25. Tran, K.A., Addala, V., Johnston, R.L., Lovell, D., Bradley, A., Koufariotis, L.T., Wood, S., Wu, S.Z., Roden, D., Al-Eryani, G., et al. (2023). Performance of tumour microenvironment deconvolution methods in breast cancer using single-cell simulated bulk mixtures. *Nat. Commun.* 14, 5758. <https://doi.org/10.1038/s41467-023-41385-5>.
26. Mahalingam, M. (2018). Laser Capture Microdissection: Insights into Methods and Applications. *Methods Mol. Biol.* 1723, 1–17. [https://doi.org/10.1007/978-1-4939-7558-7\\_1](https://doi.org/10.1007/978-1-4939-7558-7_1).
27. Aran, D. (2023). Single-Cell RNA Sequencing for Studying Human Cancers. *Annu. Rev. Biomed. Data Sci.* 6, 1–22. <https://doi.org/10.1146/annurev-biodatasci-020722-091857>.
28. Van de Sande, B., Lee, J.S., Mutasa-Gottgens, E., Naughton, B., Bacon, W., Manning, J., Wang, Y., Pollard, J., Mendez, M., Hill, J., et al. (2023). Applications of single-cell RNA sequencing in drug discovery and development. *Nat. Rev. Drug Discov.* 22, 496–520. <https://doi.org/10.1038/s41573-023-00688-4>.
29. Slyper, M., Porter, C.B.M., Ashenberg, O., Waldman, J., Droklyansky, E., Wakiro, I., Smillie, C., Smith-Rosario, G., Wu, J., Dionne, D., et al. (2020). A single-cell and single-nucleus RNA-Seq toolbox for fresh and frozen human tumors. *Nat. Med.* 26, 792–802. <https://doi.org/10.1038/s41591-020-0844-1>.
30. Cang, Z., and Nie, Q. (2020). Inferring spatial and signaling relationships between cells from single cell transcriptomic data. *Nat. Commun.* 11, 2084. <https://doi.org/10.1038/s41467-020-15968-5>.
31. Cho, M., Ahn, S., Hong, M., Bang, H., Van Vrancken, M., Kim, S., Lee, J., Park, S.H., Park, J.O., Park, Y.S., et al. (2017). Tissue recommendations for precision cancer therapy using next generation sequencing: a comprehensive single cancer center's experiences. *Oncotarget* 8, 42478–42486. <https://doi.org/10.18632/oncotarget.17199>.
32. Pagès, F., Galon, J., Dieu-Nosjean, M.-C., Tartour, E., Sautès-Fridman, C., and Fridman, W.-H. (2010). Immune infiltration in human tumors: a prognostic factor that should not be ignored. *Oncogene* 29, 1093–1102. <https://doi.org/10.1038/onc.2009.416>.
33. Stanton, S.E., and Disis, M.L. (2016). Clinical significance of tumor-infiltrating lymphocytes in breast cancer. *J. Immunother. Cancer* 4, 59. <https://doi.org/10.1186/s40425-016-0165-6>.
34. Hayashi, A., Yavas, A., McIntyre, C.A., Ho, Y.J., Erakky, A., Wong, W., Varghese, A.M., Melchor, J.P., Overholtzer, M., O'Reilly, E.M., et al. (2020). Genetic and clinical correlates of entosis in pancreatic ductal adenocarcinoma. *Mod. Pathol.* 33, 1822–1831. <https://doi.org/10.1038/s41379-020-0549-5>.
35. Mascharak, S., Guo, J.L., Foster, D.S., Khan, A., Davitt, M.F., Nguyen, A.T., Burcham, A.R., Chinta, M.S., Guardino, N.J., Griffin, M., et al. (2023). Desmoplastic stromal signatures predict patient outcomes in pancreatic ductal adenocarcinoma. *Cell Rep. Med.* 4, 101248. <https://doi.org/10.1016/j.xcrm.2023.101248>.
36. Petralia, F., Ma, W., Yaron, T.M., Caruso, F.P., Tignor, N., Wang, J.M., Charytonowicz, D., Johnson, J.L., Huntsman, E.M., Marino, G.B., et al. (2024). Pan-cancer proteogenomics characterization of tumor immunity. *Cell* 187, 1255–1277.e27. <https://doi.org/10.1016/j.cell.2024.01.027>.
37. Jhaveri, N., Ben Cheikh, B., Nikulina, N., Ma, N., Klymyshyn, D., DeRosa, J., Mihani, R., Pratapa, A., Kassim, Y., Bommakanti, S., et al. (2023). Mapping the Spatial Proteome of Head and Neck Tumors: Key Immune Mediators and Metabolic Determinants in the Tumor Microenvironment. *GEN Biotechnol.* 2, 418–434. <https://doi.org/10.1089/genbio.2023.0029>.
38. Liu, Y., DiStasio, M., Su, G., Asashima, H., Enninful, A., Qin, X., Deng, Y., Nam, J., Gao, F., Bordignon, P., et al. (2023). High-plex protein and whole transcriptome co-mapping at cellular resolution with spatial CITE-seq. *Nat. Biotechnol.* 41, 1405–1409. <https://doi.org/10.1038/s41587-023-01676-0>.
39. Zhang, D., Deng, Y., Kukanja, P., Agirre, E., Bartosovic, M., Dong, M., Ma, C., Ma, S., Su, G., Bao, S., et al. (2023). Spatial epigenome-transcriptome co-profiling of mammalian tissues. *Nature* 616, 113–122. <https://doi.org/10.1038/s41586-023-05795-1>.
40. Russell, A.J.C., Weir, J.A., Nadaf, N.M., Shabot, M., Kumar, V., Kambhampati, S., Raichur, R., Marrero, G.J., Liu, S., Balderrama, K.S., et al. (2024). Slide-tags enables single-nucleus barcoding for multimodal spatial genomics. *Nature* 625, 101–109. <https://doi.org/10.1038/s41586-023-06837-4>.
41. Cho, C.-S., Xi, J., Si, Y., Park, S.-R., Hsu, J.-E., Kim, M., Jun, G., Kang, H.M., and Lee, J.H. (2021). Microscopic examination of spatial transcriptome using Seq-Scope. *Cell* 184, 3559–3572.e22. <https://doi.org/10.1016/j.cell.2021.05.010>.
42. Fang, S., Chen, B., Zhang, Y., Sun, H., Liu, L., Liu, S., Li, Y., and Xu, X. (2023). Computational Approaches and Challenges in Spatial Transcriptomics. *Dev. Reprod. Biol.* 21, 24–47. <https://doi.org/10.1016/j.gpb.2022.10.001>.
43. Vandereyken, K., Sifrim, A., Thienpont, B., and Voet, T. (2023). Methods and applications for single-cell and spatial multi-omics. *Nat. Rev. Genet.* 24, 494–515. <https://doi.org/10.1038/s41576-023-00580-2>.
44. Stringer, C., Wang, T., Michaelos, M., and Pachitariu, M. (2021). Cellpose: a generalist algorithm for cellular segmentation. *Nat. Methods* 18, 100–106. <https://doi.org/10.1038/s41592-020-01018-x>.
45. Schmidt, U., Weigert, M., Broaddus, C., and Myers, G. (2018). Cell Detection with Star-convex Polygons. [https://doi.org/10.1007/978-3-030-00934-2\\_30](https://doi.org/10.1007/978-3-030-00934-2_30). 265–273.
46. Chen, S., Zhu, B., Huang, S., Hickey, J.W., Lin, K.Z., Snyder, M., Greenleaf, W.J., Nolan, G.P., Zhang, N.R., and Ma, Z. (2024). Integration of spatial and single-cell data across modalities with weakly linked features. *Nat. Biotechnol.* 42, 1096–1106. <https://doi.org/10.1038/s41587-023-01935-0>.
47. Brbić, M., Cao, K., Hickey, J.W., Tan, Y., Snyder, M.P., Nolan, G.P., and Leskovec, J. (2022). Annotation of spatially resolved single-cell data with STELLAR. *Nat. Methods* 19, 1411–1418. <https://doi.org/10.1038/s41592-022-01651-8>.
48. Cable, D.M., Murray, E., Zou, L.S., Goeva, A., Macosko, E.Z., Chen, F., and Irizarry, R.A. (2022). Robust decomposition of cell type mixtures in spatial transcriptomics. *Nat. Biotechnol.* 40, 517–526. <https://doi.org/10.1038/s41587-021-00830-w>.
49. Benjamin, K., Bhandari, A., Kepple, J.D., Qi, R., Shang, Z., Xing, Y., An, Y., Zhang, N., Hou, Y., Crockford, T.L., et al. (2024). Multiscale topology classifies cells in subcellular spatial transcriptomics. *Nature* 630, 943–949. <https://doi.org/10.1038/s41586-024-07563-1>.

50. Petukhov, V., Xu, R.J., Soldatov, R.A., Cadinu, P., Khodosevich, K., Moffitt, J.R., and Kharchenko, P.V. (2022). Cell segmentation in imaging-based spatial transcriptomics. *Nat. Biotechnol.* 40, 345–354. <https://doi.org/10.1038/s41587-021-01044-w>.
51. Kotliar, D., Veres, A., Nagy, M.A., Tabrizi, S., Hodis, E., Melton, D.A., and Sabeti, P.C. (2019). Identifying gene expression programs of cell-type identity and cellular activity with single-cell RNA-Seq. *Elife* 8, e43803. <https://doi.org/10.7554/elife.43803>.
52. Junnila, M.R., and de Sauvage, F.J. (2013). Influence of tumour microenvironment heterogeneity on therapeutic response. *Nature* 501, 346–354. <https://doi.org/10.1038/nature12626>.
53. Dagogo-Jack, I., and Shaw, A.T. (2018). Tumour heterogeneity and resistance to cancer therapies. *Nat. Rev. Clin. Oncol.* 15, 81–94. <https://doi.org/10.1038/nrclinonc.2017.166>.
54. Elhanani, O., Ben-Uri, R., and Keren, L. (2023). Spatial profiling technologies illuminate the tumor microenvironment. *Cancer Cell* 41, 404–420. <https://doi.org/10.1016/j.ccr.2023.01.010>.
55. Roma-Rodrigues, C., Mendes, R., Baptista, P.V., and Fernandes, A.R. (2019). Targeting Tumor Microenvironment for Cancer Therapy. *Int. J. Mol. Sci.* 20, 840. <https://doi.org/10.3390/ijms20040840>.
56. Pascual-Pasto, G., McIntyre, B., Shraim, R., Buongiovino, S.N., Erbe, A.K., Zhelev, D.V., Sadirova, S., Giudice, A.M., Martinez, D., Garcia-Gerique, L., et al. (2022). GPC2 antibody-drug conjugate reprograms the neuroblastoma immune milieu to enhance macrophage-driven therapies. *J. Immunother. Cancer* 10, e004704. <https://doi.org/10.1136/jitc-2022-004704>.
57. Zhang, X., Wang, X., Hou, L., Xu, Z., Liu, Y., and Wang, X. (2023). Nanoparticles overcome adaptive immune resistance and enhance immunotherapy via targeting tumor microenvironment in lung cancer. *Front. Pharmacol.* 14, 1130937. <https://doi.org/10.3389/fphar.2023.1130937>.
58. Hu, J., Ascierto, P., Cesano, A., Herrmann, V., and Marincola, F.M. (2024). Shifting the paradigm: engaging multicellular networks for cancer therapy. *J. Transl. Med.* 22, 270. <https://doi.org/10.1186/s12967-024-05043-8>.
59. Prat, A., Pineda, E., Adamo, B., Galván, P., Fernández, A., Gaba, L., Díez, M., Viladot, M., Arance, A., and Muñoz, M. (2015). Clinical implications of the intrinsic molecular subtypes of breast cancer. *Breast Edinb. Scotl* 24, S26–S35. <https://doi.org/10.1016/j.breast.2015.07.008>.
60. Collisson, E.A., Bailey, P., Chang, D.K., and Biankin, A.V. (2019). Molecular subtypes of pancreatic cancer. *Nat. Rev. Gastroenterol. Hepatol.* 16, 207–220. <https://doi.org/10.1038/s41575-019-0109-y>.
61. Zhao, L., Lee, V.H.F., Ng, M.K., Yan, H., and Bijlsma, M.F. (2019). Molecular subtyping of cancer: current status and moving toward clinical applications. *Briefings Bioinf.* 20, 572–584. <https://doi.org/10.1093/bib/bby026>.
62. Hwang, W.L., Jagadeesh, K.A., Guo, J.A., Hoffman, H.I., Yadollahpour, P., Reeves, J.W., Mohan, R., Drokhlyansky, E., Van Wittenbergh, N., Ashenberg, O., et al. (2022). Single-nucleus and spatial transcriptome profiling of pancreatic cancer identifies multicellular dynamics associated with neoadjuvant treatment. *Nat. Genet.* 54, 1178–1191. <https://doi.org/10.1038/s41588-022-01134-8>.
63. Keren, L., Bosse, M., Marquez, D., Angoshtari, R., Jain, S., Varma, S., Yang, S.-R., Kurian, A., Van Valen, D., West, R., et al. (2018). A Structured Tumor-Immune Microenvironment in Triple Negative Breast Cancer Revealed by Multiplexed Ion Beam Imaging. *Cell* 174, 1373–1387.e19. <https://doi.org/10.1016/j.cell.2018.08.039>.
64. Lewis, S.M., Asselin-Labat, M.-L., Nguyen, Q., Berthelet, J., Tan, X., Wimmer, V.C., Merino, D., Rogers, K.L., and Naik, S.H. (2021). Spatial omics and multiplexed imaging to explore cancer biology. *Nat. Methods* 18, 997–1012. <https://doi.org/10.1038/s41592-021-01203-6>.
65. Rao, A., Barkley, D., França, G.S., and Yanai, I. (2021). Exploring tissue architecture using spatial transcriptomics. *Nature* 596, 211–220. <https://doi.org/10.1038/s41586-021-03634-9>.
66. Hsieh, W.-C., Budiarto, B.R., Wang, Y.-F., Lin, C.-Y., Gwo, M.-C., So, D.K., Tzeng, Y.-S., and Chen, S.-Y. (2022). Spatial multi-omics analyses of the tumor immune microenvironment. *J. Biomed. Sci.* 29, 96. <https://doi.org/10.1186/s12929-022-00879-y>.
67. Zhao, T., Chiang, Z.D., Morriss, J.W., LaFave, L.M., Murray, E.M., Del Priore, I., Meli, K., Lareau, C.A., Nadaf, N.M., Li, J., et al. (2022). Spatial genomics enables multi-modal study of clonal heterogeneity in tissues. *Nature* 601, 85–91. <https://doi.org/10.1038/s41586-021-04217-4>.
68. Danenberg, E., Bardwell, H., Zanotelli, V.R.T., Provenzano, E., Chin, S.-F., Rueda, O.M., Green, A., Rakha, E., Aparicio, S., Ellis, I.O., et al. (2022). Breast tumor microenvironment structures are associated with genomic features and clinical outcome. *Nat. Genet.* 54, 660–669. <https://doi.org/10.1038/s41588-022-01041-y>.
69. Dries, R., Zhu, Q., Dong, R., Eng, C.-H.L., Li, H., Liu, K., Fu, Y., Zhao, T., Sarkar, A., Bao, F., et al. (2021). Giotto: a toolbox for integrative analysis and visualization of spatial expression data. *Genome Biol.* 22, 78. <https://doi.org/10.1186/s13059-021-02286-2>.
70. Palla, G., Spitzer, H., Klein, M., Fischer, D., Schaar, A.C., Kuemmerle, L.B., Rybakov, S., Ibarra, I.L., Holmberg, O., Virshup, I., et al. (2022). Squidpy: a scalable framework for spatial omics analysis. *Nat. Methods* 19, 171–178. <https://doi.org/10.1038/s41592-021-01358-2>.
71. Zhao, E., Stone, M.R., Ren, X., Guenther, J., Smythe, K.S., Pulliam, T., Williams, S.R., Uytengco, C.R., Taylor, S.E.B., Nghiem, P., et al. (2021). Spatial transcriptomics at subspot resolution with BayesSpace. *Nat. Biotechnol.* 39, 1375–1384. <https://doi.org/10.1038/s41587-021-00935-2>.
72. Wu, Z. (2023). Identifying spatial cellular structures with SPACE-GM. *Nat. Rev. Cancer* 23, 508. <https://doi.org/10.1038/s41568-023-00582-6>.
73. Djordjevic, A., Li, J., Fang, S., Cao, L., and Ivanovic, M. (2024). A novel variable neighborhood search approach for cell clustering for spatial transcriptomics. *GigaByte* 2024, gigabyte109. <https://doi.org/10.46471/gigabyte.109>.
74. Wu, R., Guo, W., Qiu, X., Wang, S., Sui, C., Lian, Q., Wu, J., Shan, Y., Yang, Z., Yang, S., et al. (2021). Comprehensive analysis of spatial architecture in primary liver cancer. *Sci. Adv.* 7, eabg3750. <https://doi.org/10.1126/sciadv.abg3750>.
75. Yerly, L., Pich-Bavastro, C., Di Domizio, J., Wyss, T., Tissot-Renaud, S., Cangkrama, M., Gillett, M., Werner, S., and Kuonen, F. (2022). Integrated multi-omics reveals cellular and molecular interactions governing the invasive niche of basal cell carcinoma. *Nat. Commun.* 13, 4897. <https://doi.org/10.1038/s41467-022-32670-w>.
76. Wang, Y., Chen, D., Liu, Y., Shi, D., Duan, C., Li, J., Shi, X., Zhang, Y., Yu, Z., Sun, N., et al. (2023). Multidirectional characterization of cellular composition and spatial architecture in human multiple primary lung cancers. *Cell Death Dis.* 14, 462. <https://doi.org/10.1038/s41419-023-05992-w>.
77. Liu, I., Jiang, L., Samuelsson, E.R., Marco Salas, S., Beck, A., Hack, O.A., Jeong, D., Shaw, M.L., Englinger, B., LaBelle, J., et al. (2022). The landscape of tumor cell states and spatial organization in H3-K27M mutant diffuse midline glioma across age and location. *Nat. Genet.* 54, 1881–1894. <https://doi.org/10.1038/s41588-022-01236-3>.
78. Hunter, M.V., Moncada, R., Weiss, J.M., Yanai, I., and White, R.M. (2021). Spatially resolved transcriptomics reveals the architecture of the tumor-microenvironment interface. *Nat. Commun.* 12, 6278. <https://doi.org/10.1038/s41467-021-26614-z>.
79. Greenwald, A.C., Darnell, N.G., Hoefflin, R., Simkin, D., Mount, C.W., Gonzalez Castro, L.N., Harnik, Y., Dumont, S., Hirsch, D., Nomura, M., et al. (2024). Integrative spatial analysis reveals a multi-layered organization of glioblastoma. *Cell* 187, 2485–2501.e26. <https://doi.org/10.1016/j.cell.2024.03.029>.
80. Liu, M., Ji, Z., Jain, V., Smith, V.L., Hocke, E., Patel, A.P., McLendon, R.E., Ashley, D.M., Gregory, S.G., and López, G.Y. (2024). Spatial transcriptomics reveals segregation of tumor cell states in glioblastoma and marked immunosuppression within the perinecrotic niche. *Acta Neuropathol. Commun.* 12, 64. <https://doi.org/10.1186/s40478-024-01769-0>.
81. Wieduwilt, M.J., and Moasser, M.M. (2008). The epidermal growth factor receptor family: biology driving targeted therapeutics. *Cell. Mol. Life Sci.* 65, 1566–1584.

82. Sharma, S.V., and Settleman, J. (2007). Oncogene addiction: setting the stage for molecularly targeted cancer therapy. *Genes Dev.* 21, 3214–3231.
83. Denduluri, S.K., Idowu, O., Wang, Z., Liao, Z., Yan, Z., Mohammed, M.K., Ye, J., Wei, Q., Wang, J., Zhao, L., and Luu, H.H. (2015). Insulin-like growth factor (IGF) signaling in tumorigenesis and the development of cancer drug resistance. *Genes Dis.* 2, 13–25. <https://doi.org/10.1016/j.gendis.2014.10.004>.
84. Mueller, M.M., and Fusenig, N.E. (2004). Friends or foes — bipolar effects of the tumour stroma in cancer. *Nat. Rev. Cancer* 4, 839–849. <https://doi.org/10.1038/nrc1477>.
85. Wang, X., Almet, A.A., and Nie, Q. (2023). The Promising Application of Cell-Cell Interaction Analysis in Cancer from Single-Cell and Spatial Transcriptomics. In *Seminars in cancer biology* (Elsevier).
86. Tran, M., Yoon, S., Teoh, M., Andersen, S., Lam, P.Y., Purdue, B.W., Raghubar, A., Hanson, S.J., Devitt, K., Jones, K., et al. (2022). A robust experimental and computational analysis framework at multiple resolutions, modalities and coverages. *Front. Immunol.* 13, 911873. <https://doi.org/10.3389/fimmu.2022.911873>.
87. Che, G., Yin, J., Wang, W., Luo, Y., Chen, Y., Yu, X., Wang, H., Liu, X., Chen, Z., Wang, X., et al. (2024). Circumventing drug resistance in gastric cancer: A spatial multi-omics exploration of chemo and immuno-therapeutic response dynamics. *Drug Resist. Updates* 74, 101080.
88. Valdeolivas, A., Amberg, B., Girod, N., Richardson, M., Gálvez, E.J.C., Badillo, S., Julien-Laferrière, A., Turós, D., Voith von Voithenberg, L., Wells, I., et al. (2024). Profiling the heterogeneity of colorectal cancer consensus molecular subtypes using spatial transcriptomics. *npj Precis. Oncol.* 8, 10–16. <https://doi.org/10.1038/s41698-023-00488-4>.
89. Ji, A.L., Rubin, A.J., Thrane, K., Jiang, S., Reynolds, D.L., Meyers, R.M., Guo, M.G., George, B.M., Molibrink, A., Bergenstråhlé, J., et al. (2020). Multimodal Analysis of Composition and Spatial Architecture in Human Squamous Cell Carcinoma. *Cell* 182, 497–514.e22. <https://doi.org/10.1016/j.cell.2020.05.039>.
90. Ferri-Borgogno, S., Zhu, Y., Sheng, J., Burks, J.K., Gomez, J.A., Wong, K.K., Wong, S.T.C., and Mok, S.C. (2023). Spatial Transcriptomics Depict Ligand-Receptor Cross-talk Heterogeneity at the Tumor-Stroma Interface in Long-Term Ovarian Cancer Survivors. *Cancer Res.* 83, 1503–1516. <https://doi.org/10.1158/0008-5472.CAN-22-1821>.
91. Shiau, C., Cao, J., Gong, D., Gregory, M.T., Caldwell, N.J., Yin, X., Cho, J.-W., Wang, P.L., Su, J., Wang, S., et al. (2024). Spatially resolved analysis of pancreatic cancer identifies therapy-associated remodeling of the tumor microenvironment. *Nat. Genet.* 1–13. <https://doi.org/10.1038/s41588-024-01890-9>.
92. Cang, Z., Zhao, Y., Almet, A.A., Stabell, A., Ramos, R., Plikus, M.V., Atwood, S.X., and Nie, Q. (2023). Screening cell-cell communication in spatial transcriptomics via collective optimal transport. *Nat. Methods* 20, 218–228. <https://doi.org/10.1038/s41592-022-01728-4>.
93. Li, Z., Wang, T., Liu, P., and Huang, Y. (2023). SpatialDM for rapid identification of spatially co-expressed ligand-receptor and revealing cell-cell communication patterns. *Nat. Commun.* 14, 3995. <https://doi.org/10.1038/s41467-023-39608-w>.
94. Kalluri, R., and Zeisberg, M. (2006). Fibroblasts in cancer. *Nat. Rev. Cancer* 6, 392–401. <https://doi.org/10.1038/nrc1877>.
95. Stover, D.G., Bierie, B., and Moses, H.L. (2007). A delicate balance: TGF-beta and the tumor microenvironment. *J. Cell. Biochem.* 101, 851–861. <https://doi.org/10.1002/jcb.21149>.
96. Erez, N., Truitt, M., Olson, P., Arron, S.T., and Hanahan, D. (2010). Cancer-Associated Fibroblasts Are Activated in Incipient Neoplasia to Orchestrate Tumor-Promoting Inflammation in an NF-kappaB-Dependent Manner. *Cancer Cell* 17, 135–147. <https://doi.org/10.1016/j.ccr.2009.12.041>.
97. Lu, P., Takai, K., Weaver, V.M., and Werb, Z. (2011). Extracellular matrix degradation and remodeling in development and disease. *Cold Spring Harbor Perspect. Biol.* 3, a005058. <https://doi.org/10.1101/cshperspect.a005058>.
98. Hanahan, D., and Coussens, L.M. (2012). Accessories to the crime: functions of cells recruited to the tumor microenvironment. *Cancer Cell* 21, 309–322.
99. Xu, A.M., Haro, M., Walts, A.E., Hu, Y., John, J., Karlan, B.Y., Merchant, A., and Orsulic, S. (2024). Spatiotemporal architecture of immune cells and cancer-associated fibroblasts in high-grade serous ovarian carcinoma. *Sci. Adv.* 10, eadk8805.
100. Mao, Y., Keller, E.T., Garfield, D.H., Shen, K., and Wang, J. (2013). Stromal cells in tumor microenvironment and breast cancer. *Cancer Metastasis Rev.* 32, 303–315. <https://doi.org/10.1007/s10555-012-9415-3>.
101. Bartoschek, M., Oskolkov, N., Bocci, M., Lövrot, J., Larsson, C., Sommarin, M., Madsen, C.D., Lindgren, D., Pekar, G., Karlsson, G., et al. (2018). Spatially and functionally distinct subclasses of breast cancer-associated fibroblasts revealed by single cell RNA sequencing. *Nat. Commun.* 9, 5150. <https://doi.org/10.1038/s41467-018-07582-3>.
102. Foster, D.S., Januszyk, M., Delitto, D., Yost, K.E., Griffin, M., Guo, J., Guardino, N., Delitto, A.E., Chinta, M., Burcham, A.R., et al. (2022). Multiomic analysis reveals conservation of cancer-associated fibroblast phenotypes across species and tissue of origin. *Cancer Cell* 40, 1392–1406.e7.
103. Jain, S., Rick, J.W., Joshi, R.S., Beniwal, A., Spatz, J., Gill, S., Chang, A.C.-C., Choudhary, N., Nguyen, A.T., Sudhir, S., et al. (2023). Single-cell RNA sequencing and spatial transcriptomics reveal cancer-associated fibroblasts in glioblastoma with protumoral effects. *J. Clin. Invest.* 133, e147087. <https://doi.org/10.1172/JCI147087>.
104. Peng, Z., Ye, M., Ding, H., Feng, Z., and Hu, K. (2022). Spatial transcriptomics atlas reveals the crosstalk between cancer-associated fibroblasts and tumor microenvironment components in colorectal cancer. *J. Transl. Med.* 20, 302. <https://doi.org/10.1186/s12967-022-03510-8>.
105. Cordes, L., Engler, S., Haberecker, M., Rüschoff, J.H., Moch, H., de Souza, N., and Bodenmüller, B. (2024). Cancer-associated fibroblast phenotypes are associated with patient outcome in non-small cell lung cancer. *Cancer Cell* 42, 396–412.e5. <https://doi.org/10.1016/j.ccr.2023.12.021>.
106. Zhang, S., Yuan, L., Danilova, L., Mo, G., Zhu, Q., Deshpande, A., Bell, A.T.F., Elisseeff, J., Popel, A.S., Anders, R.A., et al. (2023). Spatial transcriptomics analysis of neoadjuvant cabozantinib and nivolumab in advanced hepatocellular carcinoma identifies independent mechanisms of resistance and recurrence. *Genome Med.* 15, 72. <https://doi.org/10.1186/s13073-023-01218-y>.
107. Galon, J., and Bruni, D. (2019). Approaches to treat immune hot, altered and cold tumours with combination immunotherapies. *Nat. Rev. Drug Discov.* 18, 197–218. <https://doi.org/10.1038/s41573-018-0007-y>.
108. Hirz, T., Mei, S., Sarkar, H., Kfoury, Y., Wu, S., Verhoeven, B.M., Subtelny, A.O., Zlatev, D.V., Wszolek, M.W., Salari, K., et al. (2023). Dissecting the immune suppressive human prostate tumor microenvironment via integrated single-cell and spatial transcriptomic analyses. *Nat. Commun.* 14, 663. <https://doi.org/10.1038/s41467-023-36325-2>.
109. Zhang, Q., Abdo, R., Iosef, C., Kaneko, T., Cecchini, M., Han, V.K., and Li, S.S.-C. (2022). The spatial transcriptomic landscape of non-small cell lung cancer brain metastasis. *Nat. Commun.* 13, 5983. <https://doi.org/10.1038/s41467-022-33365-y>.
110. Platten, M., Ochs, K., Lemke, D., Opitz, C., and Wick, W. (2014). Micro-environmental clues for glioma immunotherapy. *Curr. Neurol. Neurosci. Rep.* 14, 440. <https://doi.org/10.1007/s11910-014-0440-1>.
111. Cui, X., Ma, C., Vasudevaraja, V., Serrano, J., Tong, J., Peng, Y., Delorenzo, M., Shen, G., Frenster, J., Morales, R.-T.T., et al. (2020). Dissecting the immunosuppressive tumor microenvironments in Glioblastoma-on-a-Chip for optimized PD-1 immunotherapy. *Elife* 9, e52253.
112. Ravi, V.M., Neidert, N., Will, P., Joseph, K., Maier, J.P., Kückelhaus, J., Vollmer, L., Goeldner, J.M., Behringer, S.P., Scherer, F., et al. (2022). T-cell dysfunction in the glioblastoma microenvironment is mediated by myeloid cells releasing interleukin-10. *Nat. Commun.* 13, 925. <https://doi.org/10.1038/s41467-022-28523-1>.
113. Mancusi, R., and Monje, M. (2023). The neuroscience of cancer. *Nature* 618, 467–479. <https://doi.org/10.1038/s41586-023-05968-y>.

114. Liebig, C., Ayala, G., Wilks, J.A., Berger, D.H., and Albo, D. (2009). Perineural invasion in cancer: A Review of the Literature. *Cancer* 115, 3379–3391. <https://doi.org/10.1002/cncr.24396>.
115. Schmidt, L.B., Perez-Pacheco, C., Bellile, E.L., Wu, W., Casper, K., Mierzwka, M., Rozek, L.S., Wolf, G.T., Taylor, J.M.G., and D'Silva, N.J. (2022). Spatial and Transcriptomic Analysis of Perineural Invasion in Oral Cancer. *Clin. Cancer Res.* 28, 3557–3572. <https://doi.org/10.1158/1078-0432.CCR-21-4543>.
116. Ravi, V.M., Will, P., Kueckelhaus, J., Sun, N., Joseph, K., Salié, H., Vollmer, L., Kuliesiute, U., Von Ehr, J., Benotmane, J.K., et al. (2022). Spatially resolved multi-omics deciphers bidirectional tumor-host interdependence in glioblastoma. *Cancer Cell* 40, 639–655.e13. <https://doi.org/10.1016/j.ccr.2022.05.009>.
117. Phillips, D., Matusiak, M., Gutierrez, B.R., Bhate, S.S., Barlow, G.L., Jiang, S., Demeter, J., Smythe, K.S., Pierce, R.H., Fling, S.P., et al. (2021). Immune cell topography predicts response to PD-1 blockade in cutaneous T cell lymphoma. *Nat. Commun.* 12, 6726. <https://doi.org/10.1038/s41467-021-26974-6>.
118. Allam, M., Hu, T., Lee, J., Aldrich, J., Badve, S.S., Gökmén-Polar, Y., Bhave, M., Ramalingam, S.S., Schneider, F., and Coskun, A.F. (2022). Spatially variant immune infiltration scoring in human cancer tissues. *npj Precis. Oncol.* 6, 60. <https://doi.org/10.1038/s41698-022-00305-4>.
119. Mi, H., Sivagnanam, S., Betts, C.B., Liudahl, S.M., Jaffee, E.M., Cousens, L.M., and Popel, A.S. (2022). Quantitative Spatial Profiling of Immune Populations in Pancreatic Ductal Adenocarcinoma Reveals Tumor Microenvironment Heterogeneity and Prognostic Biomarkers. *Cancer Res.* 82, 4359–4372. <https://doi.org/10.1158/0008-5472.CAN-22-1190>.
120. Shiao, S.L., Gouin, K.H., Ing, N., Ho, A., Basho, R., Shah, A., Mebane, R.H., Zitser, D., Martinez, A., Mevises, N.-Y., et al. (2024). Single-cell and spatial profiling identify three response trajectories to pembrolizumab and radiation therapy in triple negative breast cancer. *Cancer Cell* 42, 70–84.e8. <https://doi.org/10.1016/j.ccr.2023.12.012>.
121. Khodadoust, M.S., Rook, A.H., Porcu, P., Foss, F., Moskowitz, A.J., Shustov, A., Shanbhag, S., Sokol, L., Fling, S.P., Ramchurren, N., et al. (2020). Pembrolizumab in Relapsed and Refractory Mycosis Fungoides and Sézary Syndrome: A Multicenter Phase II Study. *J. Clin. Oncol.* 38, 20–28. <https://doi.org/10.1200/JCO.19.01056>.
122. Karimi, E., Yu, M.W., Maritan, S.M., Perus, L.J.M., Rezanejad, M., Sorin, M., Dankner, M., Fallah, P., Doré, S., Zuo, D., et al. (2023). Single-cell spatial immune landscapes of primary and metastatic brain tumours. *Nature* 614, 555–563. <https://doi.org/10.1038/s41586-022-05680-3>.
123. Nalio Ramos, R., Missolo-Koussou, Y., Gerber-Ferder, Y., Bromley, C.P., Bugatti, M., Núñez, N.G., Tosello Boari, J., Richer, W., Menger, L., Denizeau, J., et al. (2022). Tissue-resident FOLR2+ macrophages associate with CD8+ T cell infiltration in human breast cancer. *Cell* 185, 1189–1207.e25. <https://doi.org/10.1016/j.cell.2022.02.021>.
124. Qi, J., Sun, H., Zhang, Y., Wang, Z., Xun, Z., Li, Z., Ding, X., Bao, R., Hong, L., Jia, W., et al. (2022). Single-cell and spatial analysis reveal interaction of FAP+ fibroblasts and SPP1+ macrophages in colorectal cancer. *Nat. Commun.* 13, 1742. <https://doi.org/10.1038/s41467-022-29366-6>.
125. Matusiak, M., Hickey, J.W., van IJzendoorn, D.G.P., Lu, G., Kidziński, L., Zhu, S., Colburg, D.R.C., Luca, B., Phillips, D.J., Brubaker, S.W., et al. (2024). Spatially Segregated Macrophage Populations Predict Distinct Outcomes In Colon Cancer. *Cancer Discov.* 14, 1418–1439. <https://doi.org/10.1158/2159-8290.CD-23-1300>.
126. Ulas, E.B., Hashemi, S.M.S., Houda, I., Kaynak, A., Veltman, J.D., Fransen, M.F., Radonic, T., and Bahce, I. (2023). Predictive Value of Combined Positive Score and Tumor Proportion Score for Immunotherapy Response in Advanced NSCLC. *JTO Clin. Res. Rep.* 4, 100532. <https://doi.org/10.1016/j.jtocrr.2023.100532>.
127. Herbst, R.S., Soria, J.-C., Kowanetz, M., Fine, G.D., Hamid, O., Gordon, M.S., Sosman, J.A., McDermott, D.F., Powderly, J.D., Gettinger, S.N., et al. (2014). Predictive correlates of response to the anti-PD-L1 antibody MPDL3280A in cancer patients. *Nature* 515, 563–567. <https://doi.org/10.1038/nature14011>.
128. Bulen, B.J., Khazanov, N.A., Hovelson, D.H., Lamb, L.E., Matrana, M., Burkard, M.E., Yang, E.S.-H., Edenfield, W.J., Claire Dees, E., Onitilo, A.A., et al. (2023). Validation of Immunotherapy Response Score as Predictive of Pan-solid Tumor Anti-PD-1/PD-L1 Benefit. *Cancer Res. Commun.* 3, 1335–1349. <https://doi.org/10.1158/2767-9764.CRC-23-0036>.
129. Placke, J.-M., Kimmig, M., Griewank, K., Herbst, R., Terheyden, P., Utikal, J., Pföhler, C., Ulrich, J., Kreuter, A., Mohr, P., et al. (2023). Correlation of tumor PD-L1 expression in different tissue types and outcome of PD-1-based immunotherapy in metastatic melanoma – analysis of the DeCOG prospective multicenter cohort study ADOREG/TRIM. *EBioMedicine* 96, 104774. <https://doi.org/10.1016/j.ebiom.2023.104774>.
130. Gruoso, T., Gigoux, M., Manem, V.S.K., Bertos, N., Zuo, D., Perlitch, I., Saleh, S.M.I., Zhao, H., Souleimanova, M., Johnson, R.M., et al. (2019). Spatially distinct tumor immune microenvironments stratify triple-negative breast cancers. *J. Clin. Invest.* 129, 1785–1800. <https://doi.org/10.1172/JCI96313>.
131. Carter, J.M., Polley, M.-Y.C., Leon-Ferre, R.A., Sinnwell, J., Thompson, K.J., Wang, X., Ma, Y., Zahrieh, D., Kachergus, J.M., Solanki, M., et al. (2021). Characteristics and Spatially Defined Immune (micro)landscapes of Early-stage PD-L1-positive Triple-negative Breast Cancer. *Clin. Cancer Res.* 27, 5628–5637. <https://doi.org/10.1158/1078-0432.CCR-21-0343>.
132. Toki, M.I., Merritt, C.R., Wong, P.F., Smithy, J.W., Kluger, H.M., Syrigos, K.N., Ong, G.T., Warren, S.E., Beechem, J.M., and Rimm, D.L. (2019). High-Plex Predictive Marker Discovery for Melanoma Immunotherapy-Treated Patients Using Digital Spatial Profiling. *Clin. Cancer Res.* 25, 5503–5512. <https://doi.org/10.1158/1078-0432.CCR-19-0104>.
133. Pelka, K., Hofree, M., Chen, J.H., Sarkizova, S., Pirl, J.D., Jorgji, V., Bejnood, A., Dionne, D., Ge, W.H., Xu, K.H., et al. (2021). Spatially organized multicellular immune hubs in human colorectal cancer. *Cell* 184, 4734–4752.e20. <https://doi.org/10.1016/j.cell.2021.08.003>.
134. Alanio, C., Binder, Z.A., Chang, R.B., Nasrallah, M.P., Delman, D., Li, J.H., Tang, O.Y., Zhang, L.Y., Zhang, J.V., Wherry, E.J., et al. (2022). Immunologic Features in De Novo and Recurrent Glioblastoma Are Associated with Survival Outcomes. *Cancer Immunol. Res.* 10, 800–810. <https://doi.org/10.1158/2326-6066.CIR-21-1050>.
135. Moldoveanu, D., Ramsay, L., Lajoie, M., Anderson-Trocme, L., Lingrand, M., Berry, D., Perus, L.J.M., Wei, Y., Moraes, C., Alkallas, R., et al. (2022). Spatial mapping of the immune landscape of melanoma using imaging mass cytometry. *Sci. Immunol.* 7, eabi5072. <https://doi.org/10.1126/sciimmunol.abi5072>.
136. Sorin, M., Rezanejad, M., Karimi, E., Fiset, B., Desharnais, L., Perus, L.J.M., Milette, S., Yu, M.W., Maritan, S.M., Doré, S., et al. (2023). Single-cell spatial landscapes of the lung tumour immune microenvironment. *Nature* 614, 548–554. <https://doi.org/10.1038/s41586-022-05672-3>.
137. Andersson, A., Larsson, L., Stenbeck, L., Salmén, F., Ehinger, A., Wu, S.Z., Al-Eryani, G., Roden, D., Swarbrick, A., Borg, Å., et al. (2021). Spatial deconvolution of HER2-positive breast cancer delineates tumor-associated cell type interactions. *Nat. Commun.* 12, 6012. <https://doi.org/10.1038/s41467-021-26271-2>.
138. Meylan, M., Petitprez, F., Becht, E., Bougoün, A., Pupier, G., Calvez, A., Giglioli, I., Verkarre, V., Lacroix, G., Verneau, J., et al. (2022). Tertiary lymphoid structures generate and propagate anti-tumor antibody-producing plasma cells in renal cell cancer. *Immunity* 55, 527–541.e5. <https://doi.org/10.1016/j.immuni.2022.02.001>.
139. Liu, S., Iorgulescu, J.B., Li, S., Borji, M., Barrera-Lopez, I.A., Shanmugam, V., Lyu, H., Morriss, J.W., Garcia, Z.N., Murray, E., et al. (2022). Spatial maps of T cell receptors and transcriptomes reveal distinct immune niches and interactions in the adaptive immune response. *Immunity* 55, 1940–1952.e5. <https://doi.org/10.1016/j.immuni.2022.09.002>.
140. Ma, J., Wu, Y., Ma, L., Yang, X., Zhang, T., Song, G., Li, T., Gao, K., Shen, X., Lin, J., et al. (2024). A blueprint for tumor-infiltrating B cells across human cancers. *Science* 384, eadj4857. <https://doi.org/10.1126/science.adj4857>.
141. Hartmann, F.J., Mrdjen, D., McCaffrey, E., Glass, D.R., Greenwald, N.F., Bharadwaj, A., Khair, Z., Verberk, S.G.S., Baranski, A., Baskar, R., et al. (2021). Single-cell metabolic profiling of human cytotoxic T cells. *Nat. Biotechnol.* 39, 186–197. <https://doi.org/10.1038/s41587-020-0651-8>.
142. Wu, L., Yan, J., Bai, Y., Chen, F., Zou, X., Xu, J., Huang, A., Hou, L., Zhong, Y., Jing, Z., et al. (2023). An invasive zone in human liver cancer

- identified by Stereo-seq promotes hepatocyte–tumor cell crosstalk, local immunosuppression and tumor progression. *Cell Res.* 33, 585–603. <https://doi.org/10.1038/s41422-023-00831-1>.
143. Arora, R., Cao, C., Kumar, M., Sinha, S., Chanda, A., McNeil, R., Samuel, D., Arora, R.K., Matthews, T.W., Chandarana, S., et al. (2023). Spatial transcriptomics reveals distinct and conserved tumor core and edge architectures that predict survival and targeted therapy response. *Nat. Commun.* 14, 5029. <https://doi.org/10.1038/s41467-023-40271-4>.
  144. Liu, Y.-M., Ge, J.-Y., Chen, Y.-F., Liu, T., Chen, L., Liu, C.-C., Ma, D., Chen, Y.-Y., Cai, Y.-W., Xu, Y.-Y., et al. (2023). Combined Single-Cell and Spatial Transcriptomics Reveal the Metabolic Evolution of Breast Cancer during Early Dissemination. *Adv. Sci.* 10, 2205395. <https://doi.org/10.1002/advs.202205395>.
  145. Puram, S.V., Tirosi, I., Parikh, A.S., Patel, A.P., Yizhak, K., Gillespie, S., Rodman, C., Luo, C.L., Mroz, E.A., Emerick, K.S., et al. (2017). Single-Cell Transcriptomic Analysis of Primary and Metastatic Tumor Ecosystems in Head and Neck Cancer. *Cell* 171, 1611–1624.e24. <https://doi.org/10.1016/j.cell.2017.10.044>.
  146. Berglund, E., Maaskola, J., Schultz, N., Friedrich, S., Marklund, M., Bergenstråhlé, J., Tarish, F., Tanoglu, A., Vickovic, S., Larsson, L., et al. (2018). Spatial maps of prostate cancer transcriptomes reveal an unexplored landscape of heterogeneity. *Nat. Commun.* 9, 2419. <https://doi.org/10.1038/s41467-018-04724-5>.
  147. Xun, Z., Ding, X., Zhang, Y., Zhang, B., Lai, S., Zou, D., Zheng, J., Chen, G., Su, B., Han, L., and Ye, Y. (2023). Reconstruction of the tumor spatial microenvironment along the malignant-boundary–nonmalignant axis. *Nat. Commun.* 14, 933. <https://doi.org/10.1038/s41467-023-36560-7>.
  148. Taube, J.M., Roman, K., Engle, E.L., Wang, C., Ballesteros-Merino, C., Jensen, S.M., McGuire, J., Jiang, M., Coltharp, C., Remenik, B., et al. (2021). Multi-institutional TSA-amplified Multiplexed Immunofluorescence Reproducibility Evaluation (MITRE) Study. *J. Immunother. Cancer* 9, e002197. <https://doi.org/10.1136/jitc-2020-002197>.
  149. Berry, S., Giraldo, N.A., Green, B.F., Cottrell, T.R., Stein, J.E., Engle, E.L., Xu, H., Ogurtsova, A., Roberts, C., Wang, D., et al. (2021). Analysis of multispectral imaging with the AstroPath platform informs efficacy of PD-1 blockade. *Science* 372, eaba2609. <https://doi.org/10.1126/science.aba2609>.
  150. Liu, X., Jiang, Y., Song, D., Zhang, L., Xu, G., Hou, R., Zhang, Y., Chen, J., Cheng, Y., Liu, L., et al. (2022). Clinical challenges of tissue preparation for spatial transcriptome. *Clin. Transl. Med.* 12, e669. <https://doi.org/10.1002/ctm.2669>.
  151. Wimmer, I., Tröscher, A.R., Brunner, F., Rubino, S.J., Bien, C.G., Weiner, H.L., Lassmann, H., and Bauer, J. (2018). Systematic evaluation of RNA quality, microarray data reliability and pathway analysis in fresh, fresh frozen and formalin-fixed paraffin-embedded tissue samples. *Sci. Rep.* 8, 6351. <https://doi.org/10.1038/s41598-018-24781-6>.
  152. Jones, W., Greytak, S., Odeh, H., Guan, P., Powers, J., Bavaria, J., and Moore, H.M. (2019). Deleterious effects of formalin-fixation and delays to fixation on RNA and miRNA-Seq profiles. *Sci. Rep.* 9, 6980. <https://doi.org/10.1038/s41598-019-43282-8>.
  153. Lim, J., Chin, V., Fairfax, K., Moutinho, C., Suan, D., Ji, H., and Powell, J.E. (2023). Transitioning single-cell genomics into the clinic. *Nat. Rev. Genet.* 24, 573–584. <https://doi.org/10.1038/s41576-023-00613-w>.
  154. Cai, R., Kolabas, Z.I., Pan, C., Mai, H., Zhao, S., Kaltenecker, D., Voigt, F.F., Molbay, M., Ohn, T.-L., Vincke, C., et al. (2023). Whole-mouse clearing and imaging at the cellular level with vDISCO. *Nat. Protoc.* 18, 1197–1242. <https://doi.org/10.1038/s41596-022-00788-2>.
  155. Kiemen, A.L., Damanakis, A.I., Braxton, A.M., He, J., Laheru, D., Fishman, E.K., Chames, P., Pérez, C.A., Wu, P.-H., Wirtz, D., et al. (2023). Tissue clearing and 3D reconstruction of digitized, serially sectioned slides provide novel insights into pancreatic cancer. *Med* 4, 75–91. <https://doi.org/10.1016/j.medj.2022.11.009>.
  156. Braxton, A.M., Kiemen, A.L., Grahn, M.P., Forjaz, A., Parksong, J., Mahesh Babu, J., Lai, J., Zheng, L., Niknafs, N., Jiang, L., et al. (2024). 3D genomic mapping reveals multifocality of human pancreatic precancers. *Nature* 629, 679–687. <https://doi.org/10.1038/s41586-024-07359-3>.
  157. Erickson, A., He, M., Berglund, E., Marklund, M., Mirzazadeh, R., Schultz, N., Kvastad, L., Andersson, A., Bergenstråhlé, L., Bergenstråhlé, J., et al. (2022). Spatially resolved clonal copy number alterations in benign and malignant tissue. *Nature* 608, 360–367. <https://doi.org/10.1038/s41586-022-05023-2>.
  158. Lomakin, A., Svedlund, J., Strell, C., Gataric, M., Shmatko, A., Rukhovich, G., Park, J.S., Ju, Y.S., Dentro, S., Kleshchevnikov, V., et al. (2022). Spatial genomics maps the structure, nature and evolution of cancer clones. *Nature* 611, 594–602. <https://doi.org/10.1038/s41586-022-05425-2>.
  159. Rovira-Clavé, X., Drainas, A.P., Jiang, S., Bai, Y., Baron, M., Zhu, B., Dallas, A.E., Lee, M.C., Chu, T.P., Holzem, A., et al. (2022). Spatial epitope barcoding reveals clonal tumor patch behaviors. *Cancer Cell* 40, 1423–1439.e11. <https://doi.org/10.1016/j.ccr.2022.09.014>.
  160. Denisenko, E., de Kock, L., Tan, A., Beasley, A.B., Beilin, M., Jones, M.E., Hou, R., Muirí, D.Ó., Bilic, S., Mohan, G.R.K.A., et al. (2024). Spatial transcriptomics reveals discrete tumour microenvironments and autocrine loops within ovarian cancer subclones. *Nat. Commun.* 15, 2860. <https://doi.org/10.1038/s41467-024-47271-y>.
  161. Trapnell, C., Cacchiarelli, D., Grimsby, J., Pokharel, P., Li, S., Morse, M., Lennon, N.J., Livak, K.J., Mikkelsen, T.S., and Rinn, J.L. (2014). The dynamics and regulators of cell fate decisions are revealed by pseudotemporal ordering of single cells. *Nat. Biotechnol.* 32, 381–386. <https://doi.org/10.1038/nbt.2859>.
  162. La Manno, G., Soldatov, R., Zeisel, A., Braun, E., Hochgerner, H., Petukhov, V., Lidschreiber, K., Kastriti, M.E., Lönnberg, P., Furlan, A., et al. (2018). RNA velocity of single cells. *Nature* 560, 494–498. <https://doi.org/10.1038/s41586-018-0414-6>.
  163. Street, K., Risso, D., Fletcher, R.B., Das, D., Ngai, J., Yosef, N., Purdom, E., and Dudoit, S. (2018). Slingshot: cell lineage and pseudotime inference for single-cell transcriptomics. *BMC Genom.* 19, 477. <https://doi.org/10.1186/s12864-018-4772-0>.
  164. Pham, D., Tan, X., Balderson, B., Xu, J., Grice, L.F., Yoon, S., Willis, E.F., Tran, M., Lam, P.Y., Raghubar, A., et al. (2023). Robust mapping of spatiotemporal trajectories and cell–cell interactions in healthy and diseased tissues. *Nat. Commun.* 14, 7739. <https://doi.org/10.1038/s41467-023-43120-6>.
  165. Genshaft, A.S., Ziegler, C.G.K., Tzouanas, C.N., Mead, B.E., Jaeger, A.M., Navia, A.W., King, R.P., Mana, M.D., Huang, S., Mitsialis, V., et al. (2021). Live cell tagging tracking and isolation for spatial transcriptomics using photoactivatable cell dyes. *Nat. Commun.* 12, 4995. <https://doi.org/10.1038/s41467-021-25279-y>.
  166. Kobayashi-Kirschvink, K.J., Comiter, C.S., Gaddam, S., Joren, T., Grody, E.I., Ounadjela, J.R., Zhang, K., Ge, B., Kang, J.W., Xavier, R.J., et al. (2024). Prediction of single-cell RNA expression profiles in live cells by Raman microscopy with Raman2RNA. *Nat. Biotechnol.* 1–9. <https://doi.org/10.1038/s41587-023-02082-2>.
  167. Livermore, L.J., Isabelle, M., Bell, I.M., Scott, C., Walsby-Tickle, J., Gannon, J., Plaha, P., Vallance, C., and Ansorge, O. (2019). Rapid intraoperative molecular genetic classification of gliomas using Raman spectroscopy. *Neurooncol. Adv.* 1, vdz008. <https://doi.org/10.1093/noajnl/vdz008>.
  168. Sigle, M., Rohlfing, A.-K., Kenny, M., Scheuermann, S., Sun, N., Graeßner, U., Haug, V., Sudmann, J., Seitz, C.M., Heinemann, D., et al. (2023). Translating genomic tools to Raman spectroscopy analysis enables high-dimensional tissue characterization on molecular resolution. *Nat. Commun.* 14, 5799. <https://doi.org/10.1038/s41467-023-41417-0>.
  169. Lu, M.Y., Chen, T.Y., Williamson, D.F.K., Zhao, M., Shady, M., Lipkova, J., and Mahmood, F. (2021). AI-based pathology predicts origins for cancers of unknown primary. *Nature* 594, 106–110. <https://doi.org/10.1038/s41586-021-03512-4>.
  170. Schmauch, B., Romagnoni, A., Pronier, E., Saillard, C., Maillé, P., Calderaro, J., Kamoun, A., Sefta, M., Toldo, S., Zaslavskiy, M., et al. (2020). A deep learning model to predict RNA-Seq expression of tumours from whole slide images. *Nat. Commun.* 11, 3877. <https://doi.org/10.1038/s41467-020-17678-4>.
  171. Jia, Y., Liu, J., Chen, L., Zhao, T., and Wang, Y. (2023). THitoGene: a deep learning method for predicting spatial transcriptomics from histological

- images. *Briefings Bioinf.* 25, bbad464. <https://doi.org/10.1093/bib/bbad464>.
172. Chen, R.J., Lu, M.Y., Williamson, D.F.K., Chen, T.Y., Lipkova, J., Noor, Z., Shaban, M., Shady, M., Williams, M., Joo, B., and Mahmood, F. (2022). Pan-cancer integrative histology-genomic analysis via multimodal deep learning. *Cancer Cell* 40, 865–878.e6. <https://doi.org/10.1016/j.ccel.2022.07.004>.
173. Saillard, C., Delecourt, F., Schmauch, B., Moindrot, O., Svrcek, M., Barquier-Dupas, A., Emile, J.F., Ayadi, M., Rebours, V., de Mestier, L., et al. (2023). Pacpaint: a histology-based deep learning model uncovers the extensive intratumor molecular heterogeneity of pancreatic adenocarcinoma. *Nat. Commun.* 14, 3459. <https://doi.org/10.1038/s41467-023-39026-y>.
174. Anaya, J., Sidhom, J.-W., Mahmood, F., and Baras, A.S. (2024). Multiple-instance learning of somatic mutations for the classification of tumour type and the prediction of microsatellite status. *Nat. Biomed. Eng.* 8, 57–67. <https://doi.org/10.1038/s41551-023-01120-3>.
175. Fischer, J.R., Jackson, H.W., de Souza, N., Varga, Z., Schraml, P., Moch, H., and Bodenmiller, B. (2023). Multiplex imaging of breast cancer lymph node metastases identifies prognostic single-cell populations independent of clinical classifiers. *Cell Rep. Med.* 4, 100977. <https://doi.org/10.1016/j.xcrm.2023.100977>.
176. Hu, J., Coleman, K., Zhang, D., Lee, E.B., Kadara, H., Wang, L., and Li, M. (2023). Deciphering tumor ecosystems at super resolution from spatial transcriptomics with TESLA. *Cell Syst.* 14, 404–417.e4. <https://doi.org/10.1016/j.cels.2023.03.008>.
177. Rozenblatt-Rosen, O., Stubbington, M.J.T., Regev, A., and Teichmann, S.A. (2017). The Human Cell Atlas: from vision to reality. *Nature* 550, 451–453. <https://doi.org/10.1038/550451a>.
178. Rozenblatt-Rosen, O., Regev, A., Oberdoerffer, P., Navy, T., Hupalowska, A., Rood, J.E., Ashenberg, O., Cerami, E., Coffey, R.J., Demir, E., et al. (2020). The Human Tumor Atlas Network: Charting Tumor Transitions across Space and Time at Single-Cell Resolution. *Cell* 181, 236–249. <https://doi.org/10.1016/j.cell.2020.03.053>.
179. Lehar, J., Madissoon, E., Chevallier, J., Schiratti, J.B., Kamburov, A., Barnes, R., Haigene, C., Joy, A., Dodacki, A., Hoffmann, C., et al. (2023). MOSAIC: Multi-Omic Spatial Atlas in Cancer, effect on precision oncology. *J. Clin. Oncol.* 41, e15076. [https://doi.org/10.1200/JCO.2023.41.16\\_suppl.e15076](https://doi.org/10.1200/JCO.2023.41.16_suppl.e15076).
180. Theodoris, C.V., Xiao, L., Chopra, A., Chaffin, M.D., Al Sayed, Z.R., Hill, M.C., Mantineo, H., Brydon, E.M., Zeng, Z., Liu, X.S., and Ellinor, P.T. (2023). Transfer learning enables predictions in network biology. *Nature* 618, 616–624. <https://doi.org/10.1038/s41586-023-06139-9>.
181. Lotfollahi, M., Hao, Y., Theis, F.J., and Satija, R. (2024). The future of rapid and automated single-cell data analysis using reference mapping. *Cell* 187, 2343–2358. <https://doi.org/10.1016/j.cell.2024.03.009>.
182. He, S., Bhatt, R., Brown, C., Brown, E.A., Buhr, D.L., Chantranuvatana, K., Danaher, P., Dunaway, D., Garrison, R.G., Geiss, G., et al. (2022). High-plex imaging of RNA and proteins at subcellular resolution in fixed tissue by spatial molecular imaging. *Nat. Biotechnol.* 40, 1794–1806. <https://doi.org/10.1038/s41587-022-01483-z>.
183. Lee, J.H., Daugherty, E.R., Scheiman, J., Kalhor, R., Ferrante, T.C., Terry, R., Turczyk, B.M., Yang, J.L., Lee, H.S., Aach, J., et al. (2015). Fluorescent *in situ* sequencing (FISSEQ) of RNA for gene expression profiling in intact cells and tissues. *Nat. Protoc.* 10, 442–458. <https://doi.org/10.1038/nprot.2014.191>.
184. Ke, R., Mignardi, M., Pacureanu, A., Svedlund, J., Botling, J., Wählby, C., and Nilsson, M. (2013). In situ sequencing for RNA analysis in preserved tissue and cells. *Nat. Methods* 10, 857–860. <https://doi.org/10.1038/nmeth.2563>.
185. Chen, K.H., Boettiger, A.N., Moffitt, J.R., Wang, S., and Zhuang, X. (2015). RNA imaging. Spatially resolved, highly multiplexed RNA profiling in single cells. *Science* 348, aaa6090. <https://doi.org/10.1126/science.aaa6090>.
186. Ståhl, P.L., Salmén, F., Vickovic, S., Lundmark, A., Navarro, J.F., Magnusson, J., Giacomello, S., Asp, M., Westholm, J.O., Huss, M., et al. (2016). Visualization and analysis of gene expression in tissue sections by spatial transcriptomics. *Science* 353, 78–82. <https://doi.org/10.1126/science.aaf2403>.
187. Chen, A., Liao, S., Cheng, M., Ma, K., Wu, L., Lai, Y., Qiu, X., Yang, J., Xu, J., Hao, S., et al. (2022). Spatiotemporal transcriptomic atlas of mouse organogenesis using DNA nanoball-patterned arrays. *Cell* 185, 1777–1792.e21. <https://doi.org/10.1016/j.cell.2022.04.003>.
188. Stickels, R.R., Murray, E., Kumar, P., Li, J., Marshall, J.L., Di Bella, D.J., Arlotta, P., Macosko, E.Z., and Chen, F. (2021). Highly sensitive spatial transcriptomics at near-cellular resolution with Slide-seqV2. *Nat. Biotechnol.* 39, 313–319. <https://doi.org/10.1038/s41587-020-0739-1>.
189. Merritt, C.R., Ong, G.T., Church, S.E., Barker, K., Danaher, P., Geiss, G., Hoang, M., Jung, J., Liang, Y., McKay-Fleisch, J., et al. (2020). Multiplex digital spatial profiling of proteins and RNA in fixed tissue. *Nat. Biotechnol.* 38, 586–599. <https://doi.org/10.1038/s41587-020-0472-9>.
190. Black, S., Phillips, D., Hickey, J.W., Kennedy-Darling, J., Venkataraman, V.G., Samusik, N., Goltsev, Y., Schürch, C.M., and Nolan, G.P. (2021). CODEX multiplexed tissue imaging with DNA-conjugated antibodies. *Nat. Protoc.* 16, 3802–3835. <https://doi.org/10.1038/s41596-021-00556-8>.
191. Rivest, F., Eroglu, D., Pelz, B., Kowal, J., Kehren, A., Navikas, V., Procopio, M.G., Bordignon, P., Pérés, E., Ammann, M., et al. (2023). Fully automated sequential immunofluorescence (seqIF) for hyperplex spatial proteomics. *Sci. Rep.* 13, 16994. <https://doi.org/10.1038/s41598-023-43435-w>.
192. Jarosch, S., Köhlen, J., Sarker, R.S.J., Steiger, K., Janssen, K.-P., Christians, A., Hennig, C., Holler, E., D'Ipoltto, E., and Busch, D.H. (2021). Multiplexed imaging and automated signal quantification in formalin-fixed paraffin-embedded tissues by ChipCytometry. *Cell Rep. Methods* 1, 100104. <https://doi.org/10.1016/j.crmeth.2021.100104>.
193. Larroquette, M., Guegan, J.-P., Besse, B., Cousin, S., Brunet, M., Le Moulec, S., Le Loarer, F., Rey, C., Soria, J.-C., Barlesi, F., et al. (2022). Spatial transcriptomics of macrophage infiltration in non-small cell lung cancer reveals determinants of sensitivity and resistance to anti-PD1/PD-L1 antibodies. *J. Immunother. Cancer* 10, e003890. <https://doi.org/10.1136/jitc-2021-003890>.
194. Hammerl, D., Martens, J.W.M., Timmermans, M., Smid, M., Trapman-Jansen, A.M., Fockens, R., Isaeva, O.I., Voorwerk, L., Balcioglu, H.E., Wijers, R., et al. (2021). Spatial immunophenotypes predict response to anti-PD1 treatment and capture distinct paths of T cell evasion in triple negative breast cancer. *Nat. Commun.* 12, 5668. <https://doi.org/10.1038/s41467-021-25962-0>.
195. Wang, X.Q., Danenberg, E., Huang, C.-S., Egle, D., Callari, M., Bermejo, B., Dugo, M., Zamagni, C., Thill, M., Anton, A., et al. (2023). Spatial predictors of immunotherapy response in triple-negative breast cancer. *Nature* 621, 868–876. <https://doi.org/10.1038/s41586-023-06498-3>.
196. Moutafi, M.K., Molero, M., Martinez Morilla, S., Baena, J., Vathiotis, I.A., Gavrielatou, N., Castro-Labrador, L., de Garibay, G.R., Adradas, V., Orive, D., et al. (2022). Spatially resolved proteomic profiling identifies tumor cell CD44 as a biomarker associated with sensitivity to PD-1 axis blockade in advanced non-small-cell lung cancer. *J. Immunother. Cancer* 10, e004757. <https://doi.org/10.1136/jitc-2022-004757>.
197. Sadeghirad, H., Liu, N., Monkman, J., Ma, N., Cheikh, B.B., Jhaveri, N., Tan, C.W., Warkiani, M.E., Adams, M.N., Nguyen, Q., et al. (2023). Compartmentalized spatial profiling of the tumor microenvironment in head and neck squamous cell carcinoma identifies immune checkpoint molecules and tumor necrosis factor receptor superfamily members as biomarkers of response to immunotherapy. *Front. Immunol.* 14, 1135489. <https://doi.org/10.3389/fimmu.2023.1135489>.
198. Gil-Jimenez, A., van Dijk, N., Vos, J.L., Lubeck, Y., van Montfoort, M.L., Peters, D., Hooijberg, E., Broeks, A., Zuur, C.L., van Rhijn, B.W.G., et al. (2024). Spatial relationships in the urothelial and head and neck tumor microenvironment predict response to combination immune checkpoint inhibitors. *Nat. Commun.* 15, 2538. <https://doi.org/10.1038/s41467-024-46450-1>.
199. Sun, Y., Wu, P., Zhang, Z., Wang, Z., Zhou, K., Song, M., Ji, Y., Zang, F., Lou, L., Rao, K., et al. (2024). Integrated multi-omics profiling to dissect the spatiotemporal evolution of metastatic hepatocellular carcinoma. *Cancer Cell* 42, 135–156.e17. <https://doi.org/10.1016/j.ccel.2023.11.010>.

200. Nirmal, A.J., Maliga, Z., Vallius, T., Quattrochi, B., Chen, A.A., Jacobson, C.A., Pelletier, R.J., Yapp, C., Arias-Camison, R., Chen, Y.-A., et al. (2022). The Spatial Landscape of Progression and Immunoediting in Primary Melanoma at Single-Cell Resolution. *Cancer Discov.* 12, 1518–1541. <https://doi.org/10.1158/2159-8290.CD-21-1357>.
201. Yofe, I., Shami, T., Cohen, N., Landsberger, T., Sheban, F., Stoler-Barak, L., Yalin, A., Phan, T.S., Li, B., Monteran, L., et al. (2023). Spatial and Temporal Mapping of Breast Cancer Lung Metastases Identify TREM2 Macrophages as Regulators of the Metastatic Boundary. *Cancer Discov.* 13, 2610–2631. <https://doi.org/10.1158/2159-8290.CD-23-0299>.
202. Li, R., Ferdinand, J.R., Loudon, K.W., Bowyer, G.S., Laidlaw, S., Muyas, F., Mamanova, L., Neves, J.B., Bolt, L., Fasouli, E.S., et al. (2022). Mapping single-cell transcriptomes in the intra-tumoral and associated territories of kidney cancer. *Cancer Cell* 40, 1583–1599.e10. <https://doi.org/10.1016/j.ccr.2022.11.001>.